STABILITY OF THIN PIPES WITH AN INTERNAL FLOW

STABILITY OF THIN PIPES WITH AN INTERNAL FLOW

by

B. Myklatun

A Thesis

Submitted to the Faculty of Graduate Studies

in Partial Fulfilment of the Requirements

for the Degree

Master of Engineering

McMaster University

September, 1973

Master of Engineering (1973) McMaster University
(Mechanical Engineering) Hamilton, Ontario

Title: Stability of Thin Pipes with an Internal Flow

Author: B. Myklatun, B.Sc (Heriot-Watt University Edinburgh, Scotland)

Supervisor: Dr. D. S. Weaver

Number of Pages: iv, 63

Scope and Content:

The stability behaviour of a thin clamped-ended pipe with an internal flow is determined. Classical potential flow theory is used to determine the unsteady fluid forces and the motion of the pipe is represented by the Flugge-Kempner equation. The solution is obtained using Fourier integral theory and the method of Galerkin.

Theoretical results are compared with experiments as well as previous work.

TABLE OF CONTENTS

ACKNOWLEDGMENTS

The author gratefully acknowledges the assistance and guidance of Dr. D. S. Weaver in planning, and carrying out this work. Without his encouragement this work would not have been possible.

In addition, the author is indebted to Dr. R. Tennyson and J. Young of the Institute of Aerospace Studies at the University of Toronto for making the experimental tubes. I am also indebted to my wife for reading proof and her patience and understanding during this time.

The financial support of the National Research Council of Canada is also gratefully acknowledged.

ABSTRACT

This thesis has the objective of establishing the stability behaviour of a thin clamped-ended pipe with internal flow. The unsteady fluid forces on the pipe wall is determined by using classical potential flow theory for an incompressible, inviscid fluid and the motion of the pipe is represented by Flugge-Kempner shell equation. The solution is obtained using Fourier integral theory and the method of Galerkin. It is found that the pipe becomes unstable statically in a mode being comprised of one axial half-wave and a number of circumferential waves depending on the length and thickness ratios. For the limiting case of a relatively long thin pipe the mode of instability is the first beam mode and a particular simple expression is found for the critical flow velocity. Furthermore, the mode shape at instability always corresponds to that of the lowest natural frequency of the pipe.

The theoretical results are compared with experiments and previous work developed by different methods and the agreement found is good.

CHAPTER 1

INTRODUCTION

1.1. General

The problem of the dynamic behaviour of a flexible tube with an internal or external flowing fluid is of fundamental interest and importance in a variety of engineering applications. Examples are found in the bending oscillations in a long pipe as observed in oil pipe lines [1], dynamic or static instability of steel conduits for hydro-electric plants [2] and liquid fuel propellant lines [3]. External flow on cylindrical shells as in the cooling flow of a nuclear reactor causes oscillation of the fuel bundles [4], [5]. The latter phenomenon is mainly the result of hydrodynamic forces caused by unsteady fluid flow and is of particular interest in boiling water reactors. Similar problems exist in the steam generators presently used in the CANDU-PHW* reactors, where the two-phase axial flow on the shell side of the steam generator causes the heated tubes carrying the heavy water to vibrate. Other examples are the numerous observed instabilities of the shell components of aircraft at a velocity both above and below the speed of sound [6]. The Korotkoff sounds in the arterial system occuring during strenuous exercises is a similar instability [7].

---

* CANDU-PHW: CANADA Deuterium Uranium - Pressurized Heavy Water

The above problems with instabilities of shells due to fluid forces have received considerable analytical and experimental attention in recent years. The increasing desirability of higher fluid velocities coupled with more flexible structures will require the design engineer to have knowledge of the above problems. He must be in a position to predict their occurrence for their existence is inevitable.

1.2. Theoretical Approach

The phenomena of flow induced instability of shells as encountered above are characterized by the interaction of elastic, inertia and hydrodynamic or aerodynamic forces and falls within the general classification of "hydroelasticity" or "aeroelasticity". In hydro-aeroelastic problems the operative forces are nonconservative since they cannot be derived from a potential function, i.e., they are dependent on the path travelled. This results in the possibility of the shell extracting energy from the fluid in such a way that it becomes unstable.

In examining the stability of problems involving nonconservative forces it has been found that it is not always sufficient to use the static or Euler method, which looks for the smallest force under which the system can be in equilibrium not only in its original configuration but also in an infinitely close configuration. An alternative is to use the dynamic method which involves the investigation of the stability of

infinitesimal oscillations of the system about its equilibrium position. The critical force by this criterion is the smallest force under which a small disturbance will increase with time. In certain problems the stability may be lost in a static sense in which case the Euler method would give the correct answer. However this is difficult to determine in advance and since a static method cannot predict dynamic instability a dynamic method should always be used.

The instabilities of shells containing flowing fluid are different depending on the boundary conditions, the length and the wall thickness of the shell. For fixed boundaries and $\ell/a > a/h$, where ℓ is the length of the shell, a the radius and h the wall thickness, the instability is similar to the buckling of an "Euler" column at a sufficiently high flow velocity [8]. The mode of instability is always the first beam mode. The analytical approach in establishing the buckling boundary or "divergence" as it is called in aeroelasticity is by using a static method. However before it was established that the stability was lost in a static sense, a dynamic method was used. A dynamic solution is of the form

$$W(x_j,t) = Y(x_j)\, e^{i\omega t} \tag{1.1}$$

where ω is the natural frequency of the shell. The analysis consists in determination of the natural frequencies as a function of fluid velocity. For sufficiently small flow velocities the frequencies are real and the system is thus

stable under an arbitrary small disturbance, exhibiting bounded harmonic oscillations. As the velocity is increased, instability occurs when the natural frequency becomes zero (buckling) at the critical flow velocity. For a cantilevered shell a dynamic method is necessary to establish the instability boundary. The natural frequency for a cantilevered shell is of the form $\omega = R + iS$ at a sufficiently high flow velocity. The dynamic solution is now of the form

$$W(x_j,t) = Y(x_j)\ e^{iRt}\ e^{-St} \qquad (1.2)$$

As the flow velocity increases the imaginary part of the complex frequency decreases and eventually becomes negative at which point the system becomes unstable by exponentially growing oscillations. However due to nonlinear elastic constraints the amplitude of oscillation will be of finite magnitude. The boundary of instability occurs when the imaginary part S is zero and the frequency of oscillation R is finite. This kind of instability has been given the name "Flutter" in the field of aeroelasticity.

For a short thin shell where $\ell/a < a/h$ the instabilities are associated with circumferential deformation of the shell wall. In establishing the stability boundary a differential equation of motion of the cylindrical shell is used. The dynamic solution is of the form

$$W(x_j,\theta,t) = Y(x_j)\cos n\theta\ \ e^{i\omega t} \qquad (1.3)$$

where cos nθ represents the variation in the radial displacement

of the cylindrical wall, n being the circumferential mode number. In addition to the instabilities reported for the longer shell, circumferential oscillation now exists, at sufficiently high flow velocities.

1.3. Statement of Problem

The instabilities of pipes containing a flowing fluid have been analytically investigated by a number of authors [1], [2], [9]. However in the area of circumferential instabilities, analytical solution have only been reported by two authors [10], [11]. In this thesis the behaviour of a clamped ended cylindrical shell is examined with particular attention paid to divergence boundaries both for circumferential and beam like instabilities and the relationship of the natural frequencies at zero flow velocities to the critical mode shape. The solution is obtained using Fourier Integral theory and the method of Galerkin, and is similar to that used in reference [11] which examines pinned-ended shells. Although this approach is not without shortcomings (discussed below), it offers the advantage that the resulting algebraic equations facilitate a complete parametric study and allow a simple analytical expression to be obtained for the limiting case of a long thin shell. In addition, the flow condition at the ends of the length of shell being considered are quite different from those implicit in the travelling wave type analysis of reference [10]. This may have appreciable influence when the shells are short.

The theoretical predictions are compared with experiments as well as with previous results.

CHAPTER 2

HISTORICAL REVIEW

The early study of the dynamic stability of pipes conveying fluids was initiated by the observed transverse vibration in the trans-Arabian pipeline. The trans-Arabian pipeline is a 30 inch diameter pipe which is supported at 66 ft intervals and has about 20 inches clearance between the bottom of the pipe and the ground. At a wind velocity of approximately 20 m.p.h. the pipe was observed to vibrate with a frequency of vibration of approximately 1.2 cycles per sec and a maximum amplitude of vibration of 3/16 inches at the mid span. During vibrations the adjacent spans moved in opposite directions with nodes at the supports.

The first analytical investigation of the above phenomena was done by Ashley and Haviland [1]. Using a beam theory they found that the flow of fluid in such a pipeline produces marked damping tendencies and thus reduces the severity of loading encountered. Further, their calculations showed that the frequency of oscillation stayed constant while the damping increased rapidly over the flow range considered. Their analysis, by treating the flux of the fluid in the pipe to induce a shear force at each section due to the lateral motion of the pipe, underestimated the influence of the fluid velocity and their differential equation of motion for the pipeline and their

findings have been disputed by later authors. However their general approach is of value and their main error lies in the approach to find a solution to the differential equation of motion.

The first solutions which correctly predicted the effect of fluid flow on vibration frequency and static (buckling) instability were given by G. W. Housner [2] and F. I. N. Niordson [3]. They showed that the fluids have no beneficial effect upon the vibration of the pipe. The fluid velocity causes a dynamic coupling of the simple modes of vibration so that normal modes of vibration are of complex shape with 90^{o} out of phase components. Also, in contrast to the results of Ashley and Haviland, the frequency of vibration of the pipe decreases with increased fluid velocity until it becomes equal to zero where static divergence occurs. This work revised most of that done by Ashley and Haviland and the differential equation of motion derived for a pipe conveying fluid has been verified and used by later authors as their starting point for investigating different configurations. Niordson also formulated the problem in terms of the shell equation but did not proceed to solve it.

These first substantial contributors to the solution of the stability of a pipe conveying fluid had difficulty in obtaining an exact solution to the differential equation of motion which is not easily obtained without an electronic computer. Ashley and Haviland approached the solution by using a polynomial which approximately represented the mode shape and

satisfied the equation of motion and the boundary conditions (pinned-pinned ends). Housner regarded the distorted modes (also for the special case of pinned-pinned ends) as a linear combination of appropriate quantities of each of the classical normal modes for an Euler beam. By disregarding the contribution from classical modes higher than the second a frequency equation was obtained. A paper by Long [12] used an iterative procedure based on the method used by Ashley and Haviland but included more terms in the mode shape polynomial. After the introduction of the electronic computer authors like Nagubswaran and Williams [4] have developed "exact" solutions for the natural frequencies and mode shapes. Their results have verified the work done by earlier authors and supplemented the data available. They were also the first to report on the influence of internal pressure on the natural frequencies of vibration. As the pressure increases the natural frequencies decrease until buckling occurs.

T. B. Benjamin [13] dealing with the general dynamic problem of a chain of articulated pipes conveying fluid was the first to report on the phenomena of unstable oscillation which is possible when such a system possesses one free end. He produced a complete theory supported by experiments for articulated pipes. Although his theoretical model possesses only a few degrees of freedom it demonstrated all the essential features of this form of instability. Benjamin showed that when the pipe is vertical both unstable oscillation and buckling

instability are possible in general, whereas when the motion is confined to a horizontal plane buckling cannot occur, i.e., when gravity forces are insignificant.

The work of Benjamin was extended to cover instabilities of a continuous system by Gregory and Paidoussis [14]. They found that a tubular cantilever containing fluid developed unstable oscillation at a certain fluid velocity, which grows into lateral oscillation of large amplitude. The system was shown to become unstable first in its second mode. The system could however be unstable in other modes, i.e., by increasing the fluid velocity the system became unstable in another mode. The mode shapes for higher fluid velocities were more complex and contained components of several normal modes. They verified their theory by doing experiments on rubber tubes conveying water and air. Some discrepancies were found however near the critical flow velocities. As they used a linear theory which applies only to small oscillation, they suggested that a non-linear theory should be used near the critical fluid velocities. To predict the boundary of instabilities however their linear theory gave good results.

In the above papers two different systems have been considered. Depending on the support at the ends, the systems may be grouped as conservative systems and non-conservative systems [15]. It has been shown by Housner [9] and Long [12] that the conservative system which has no displacement at the ends loses stability only by buckling while

the non-conservative system represented by a cantilever tube, studied by Benjamin [13] and Gregory and Paidoussis [14] loses stability only by unstable oscillation. In a paper by Shoei-Sheng Chen [15] consideration is given to the transition mechanism of these two instabilities. For this purpose he studied a cantilevered tube conveying fluid with a displacement spring attached to its free end. The variation in the spring constant permits carrying out gradual transition from unstable oscillation instability to buckling instability. It was shown that depending on the spring constant, the tube lost stability by unstable oscillation, buckling or both with multiple stable and unstable range of flow velocities. However, buckling can only occur above a critical value of the spring constant. Thus the types of instabilities apparently are associated with the boundary conditions.

All of the above authors considered the shell as a beam and its motion as being exclusively lateral, i.e., the so-called first circumferential or beam-type modes. Recently Paidoussis and Denise [9] and Weaver and Unney [10] have investigated the so-called circumferential type of instabilities of cylindrical shells conveying fluid. This circumferential instability was apparently first reported in 1969 by Paidoussis and Denise [7] when conducting experiments with vertical cantilevers made of rubber conveying low pressure air. They observed that if the cantilevers had sufficiently thick walls the only form of instability was that of unstable oscillation

which has been reported earlier. However if the rubber cantilever tubes had fairly thin walls and were sufficiently short so that they remained stable with respect to the lateral instability to fairly high flow velocities, another form of instability occurred spontaneously at a certain critical flow velocity. The cantilever was seen to vibrate in the second circumferential mode and generate a shrill sound. For longer tubes this instability was superimposed on the lateral one. In their theoretical analysis Paidoussis and Denise used the three Flugge equations of motion for a cylindrical shell and the fluid pressure on the shell wall was derived using classical potential theory. They solved the differential equation by assuming a travelling wave solution. This has some shortcomings as it leads to a characteristic equation being transcendental in the wave number. The complete solution is therefore an infinite series and requires an infinite number of boundary conditions to establish the frequency equation. Therefore they have to disregard the contribution of mode shapes higher than the number of boundary conditions. Further, their solution of the frequency equation is rather cumbersome, as an iterative procedure must be used.

Weaver and Unny have also used the Flugge equation of motion for a cylindrical shell, but in a form that contains only the radial displacement. This simpler form of the shell equation was derived by Kempner [16], by making the assumption that the axial and circumferential inertias are negligible and that the shell is thin. The fluid forces were derived

from classical potential theory and the solution was obtained using Fourier Integral theory and the method of Galerkin. Although this approach requires the numerical evaluation of several improper integrals, the complex frequency and thereby the stability behaviour may be examined by the exact solution of relatively simple algebraic equations. The behaviour reported was qualitatively the same as that given by Paidoussis and Donise.

CHAPTER 3

THEORETICAL INVESTIGATION

3.1. General

The mathematical model used in this thesis to establish the instability boundaries of a clamped ended cylindrical shell subjected to hydrodynamic forces, is essentially of the same form as that developed by Weaver and Unny [11], [17] for a flat plate and a pinned ended cylindrical shell respectively. Only the general outline of this model is therefore presented here.

The important characteristics of this model are as follows: Only the limiting case of small oscillation is considered, i.e., the theory is linearized and is therefore only capable of describing the behaviour of the system up to and including the threshold of instability. However, the instability boundary given by a linearized analysis is the same as that given by a nonlinear analysis. This is given in a theorem by Liapunov which states that if the behaviour of a linearized system is asymptotically stable, or unstable, then the stability boundary of this system is the same as that derived by a nonlinear analysis [18]. Furthermore the shell is considered to be thin, and the shell material to be purely elastic homogeneous and isotopic. The fluid forces are derived from potential flow theory: i.e., on the assumption that the fluid is inviscid irrotational and incompressible.

3.2. Theoretical Development

The specific configuration studied is shown in Figure 3.1 together with the first couple of circumferential mode shapes. The differential equation of motion used for the shell is essentially the form of Flugge equation given by Kempner [16]. Kempner showed that the three Flugge equations which contain expressions for the axial, circumferential and radial displacements can be expressed in a form similar to the Donnell equation for a shell containing only the radial displacement, and the axial and circumferential displacements are absent from it. When the assumption is made that the shell is thin, $\frac{1}{12}\left(\frac{h}{R}\right)^2 << 1$, a somewhat simplified equation is obtained. Hoff [19] has recommended the use of this equation over that of Donnell unless the shell is very short and a number of circumferential modes are considered $n > 4$.

$$D\left\{\nabla^4 w + \frac{1}{R^4}\nabla^{-4}\left[\frac{12(1-\nu^2)}{\left(\frac{h}{R}\right)^2}\frac{\partial^4 w}{\partial x^4} + \frac{2(2-\nu)}{R^2}\frac{\partial^4 w}{\partial x^2 \partial \theta^2} + \frac{1}{R^4}\frac{\partial^4 w}{\partial \theta^4}\right.\right.$$

$$\left.\left. + 2\nu R^2\frac{\partial^6 w}{\partial x^6} + 6\frac{\partial^6 w}{\partial x^4 \partial \theta^2} + \frac{2(4-\nu)}{R^2}\frac{\partial^6 w}{\partial x^2 \partial \theta^4} + \frac{2}{R^4}\frac{\partial^6 w}{\partial \theta^6}\right]\right\} + \rho_m h\frac{\partial^2 w}{\partial t^2} = p_d \qquad (3.1)$$

where w is the radial displacement of the shell,

D is the flexural stiffness,

ρ_m is the density of the shell material and

p_d is the dynamic pressure of the fluid on the shell resulting from the motion of the latter.

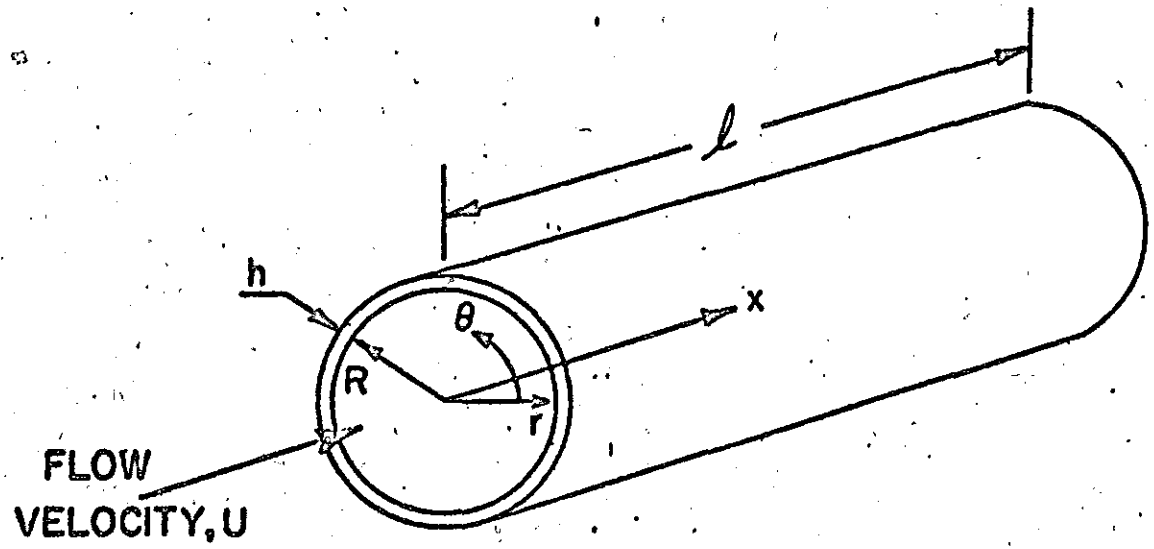

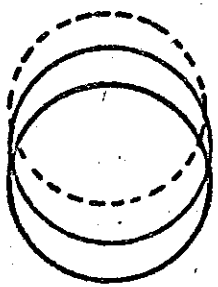

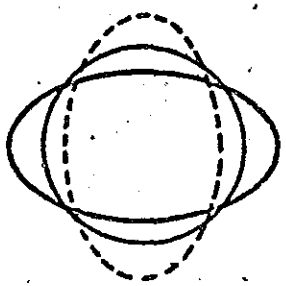

FIG. 3.1

For clamped ends, the shell boundary conditions are given by:

$$w(0) = w(\ell) = 0$$
$$\frac{\partial w(0)}{\partial x} = \frac{\partial w(\ell)}{\partial x} = 0 \qquad (3.2)$$

The dynamic pressure on the shell wall as a result of the shell wall's vibration can be determined by solving a boundary value problem for the velocity potential of the fluid flow. The fluid inside the shell with velocity vectors, V_x, V_θ, V_r, density ρ and pressure p is governed by the following system of equations:

Continuity equation:

$$\frac{\partial \rho}{\partial t} + \frac{\partial(\rho V_x)}{\partial x} + \frac{1}{r}\frac{\partial(\rho V_\theta)}{\partial \theta} + \frac{\partial(\rho V_r)}{\partial r} + \frac{\rho V_r}{r} = 0 \qquad (3.3)$$

which is derived by the condition of mass conservation.

Euler equation of motion:

$$\frac{\partial V_x}{\partial t} + \frac{\partial(V_x^2)}{\partial x} + \frac{1}{r}\frac{\partial(V_x V_\theta)}{\partial \theta} + \frac{\partial(V_x V_r)}{\partial r} + \frac{V_x V_r}{r} = -\frac{1}{\rho}\frac{\partial p}{\partial x}$$

$$\frac{\partial V_\theta}{\partial t} + \frac{\partial(V_\theta V_x)}{\partial x} + \frac{1}{r}\frac{\partial(V_\theta^2)}{\partial \theta} + \frac{\partial(V_\theta V_r)}{\partial r} + \frac{2V_\theta V_r}{r} = -\frac{1}{\rho r}\frac{\partial p}{\partial \theta} \qquad (3.4)$$

$$\frac{\partial V_r}{\partial t} + \frac{\partial(V_r V_x)}{\partial x} + \frac{1}{r}\frac{\partial(V_r V_\theta)}{\partial \theta} + \frac{\partial(V_r^2)}{\partial r} + \frac{V_r^2}{r} = -\frac{1}{\rho}\frac{\partial p}{\partial r}$$

The velocity inside the shell is everywhere close to the free stream velocity U. We can therefore express the

total velocity at any point in the flow as the free stream velocity plus a small perturbation velocity, indicated by primes.

$$\begin{aligned} V_x &= U + V'_x \qquad V'_x/U \ll 1 \\ V_\theta &= V'_\theta \qquad V'_\theta/U \ll 1 \\ V_r &= V'_r \qquad V'_r/U \ll 1 \end{aligned} \tag{3.5}$$

Using (3.4) and (3.5) and linearizing gives:

$$\begin{aligned} \frac{\partial V'_x}{\partial t} + \frac{1}{2}\frac{\partial}{\partial x}(U^2 + 2UV'_x) &= -\frac{1}{\rho}\frac{\partial p}{\partial x} \\ \frac{\partial V'_\theta}{\partial t} + U\frac{\partial}{\partial x}V'_\theta &= -\frac{1}{\rho r}\frac{\partial p}{\partial \theta} \\ \frac{\partial V'_r}{\partial t} + U\frac{\partial}{\partial x}V'_r &= -\frac{1}{\rho}\frac{\partial p}{\partial r} \end{aligned} \tag{3.6}$$

If the velocity field (V'_x, V'_θ, V'_r) is irrotational, i.e., that the fluid particles have zero angular momentum about their own centre of gravity, it can be expressed in terms of a perturbation velocity potential defined as:

$$\begin{aligned} \frac{\partial \phi}{\partial x} &= V_x - U = V'_x \\ \frac{1}{r}\frac{\partial \phi}{\partial \theta} &= V'_\theta \\ \frac{\partial \phi}{\partial r} &= V'_r \end{aligned} \tag{3.7}$$

Substituting (3.7) in (3.6) and integrating with respect to x gives an arbitrary function of time f(t), which has no effect upon the flow pattern. For parallel streamlines of velocity U, f(t) can be set equal to $\frac{U^2}{2}$ and the pressure on the shell wall is found to be:

$$p_d|_{r=R} = -\rho_o \left(\frac{\partial \phi}{\partial t} + U \frac{\partial \phi}{\partial x}\right) \tag{3.8}$$

This is the unsteady Bernoulli equation.

The determining equation for the perturbation velocity potential ϕ is found by substituting the expression for the velocity field (3.7) into (3.3). For incompressible fluid this operation yields the Laplace equation in cylindrical co-ordinates.

$$\frac{\partial^2 \phi}{\partial r^2} + \frac{1}{r}\frac{\partial \phi}{\partial r} + \frac{1}{r^2}\frac{\partial^2 \phi}{\partial \theta^2} + \frac{\partial^2 \phi}{\partial x^2} = 0, \qquad r \leq R \tag{3.9}$$

This is the continuity equation for an incompressible, irrotational, inviscid fluid.

To solve the Laplace equation for the problem of interest here it is necessary to establish the appropriate boundary conditions. The condition at the shell wall is simply that the perpendicular component of the fluid velocity is fixed to the wall's motion, as no fluid particle can pass through the shell wall. The equation for the shell wall is given by:

$$F(x,r,\theta,t) = 0 \tag{3.10}$$

the boundary condition is:

$$\frac{dF}{dt} = \frac{\partial F}{\partial t} + V_x \frac{\partial F}{\partial x} + V_r \frac{\partial F}{\partial r} + \frac{V_\theta}{r} \frac{\partial F}{\partial \theta} = 0 \qquad (3.11)$$

In other words the material rate of change of the value of the function F is zero when we follow a particle that continuously touches the surface F = 0.

As the shell wall lies very close to distance r from origin, r may be separated out from equation (3.10) and the equation for the surface then takes the form:

$$F(x,\theta,r,t) \sim w(x,\theta,t) \qquad (3.12)$$

and the boundary condition is:

$$V_r - \frac{\partial w}{\partial t} + V_x \frac{\partial w}{\partial x} + \frac{V_\theta}{r} \frac{\partial w}{\partial \theta} = 0 \qquad (3.13)$$

using (3.5) and (3.7) and linearizing since the perturbation velocities are assumed to be very small, the boundary condition becomes:

$$\left.\frac{\partial \phi}{\partial r}\right|_{r=R} = \frac{\partial w}{\partial t} + U \frac{\partial w}{\partial x}, \quad 0 < x \leq \ell \qquad (3.14)$$

For the rigid cylinder adjacent to the shell the normal fluid velocity must be equal to zero, so that equation (3.14) reduces to:

$$\left.\frac{\partial \phi}{\partial r}\right|_{r=R} = 0, \quad 0 > x > \ell \qquad (3.15)$$

3.3. Problem Solution

An assumed solution for the radial displacement of the shell must satisfy all the boundary conditions (3.2) and be in a simple enough form to make the problem tractable. This is not very easy for the clamped ended shell considered. A solution assumed was a polynomial of the form:

$$w(x,\theta,t) = \sum_{p=0}^{\infty} A_p \frac{(\ell-x)^2 x^{p+2}}{\ell^{4+p}} \cos n\theta \, e^{i\omega t} \qquad (3.16)$$

Although using only the first two terms of the infinite series, this results in a very lengthy expression for the dynamic pressure. Also this leads to significant computational difficulty when using this expression in the shell equation (3.1). As a result the solution adopted is:

$$w(x,\theta,t) = \sum_{p=1} C_p \cos n\theta \, (1-\cos \frac{2p\pi x}{\ell}) \, e^{i\omega t} \qquad (3.17)$$

where p is the number of axial half waves and n is the number of circumferential waves. This solution has the unfortunate characteristic that it only represents odd axial mode shapes. Therefore it cannot predict "flutter" instability as this is produced by fluid dynamic coupling of odd and even modes. However, it has been shown by Paidoussis and Denise [10] and Weaver and Unny [11] that flutter occurs only for flow velocities higher than required for static buckling in the first axial mode and the latter is satisfactorily represented by equation (3.17). For the purpose of establishing the stability boundary, equation (3.17) is therefore quite useful. Since the instability

investigated is of the divergence type the problem could be analyzed by using a "static method". However, the solution will be obtained using the "dynamic method" since it is of interest to compare the mode shape of the fundamental frequency at zero flow velocity with that at the critical divergence velocity.

The Laplace equation (3.9) and the boundary condition (3.14) represent a boundary value problem in the perturbation velocity potential ϕ. If the vibration of the shell is assumed harmonic, the perturbation velocity potential takes the form:

$$\phi(x,r,\theta,t) = \bar{\phi}(x,r,\theta)\, e^{i\omega t} \qquad (3.18)$$

The problem of finding the dynamic pressure on the shell wall reduces therefore to determining the perturbation velocity potential $\bar{\phi}$. Using the method of separation of variables, let

$$\phi = R(r)\,\theta(\theta)\,X(x) \qquad (3.19)$$

and substituting (3.19) into (3.9) gives

$$\frac{1}{R}\left\{\frac{d^2R}{dr^2} + \frac{1}{r}\frac{dR}{dr}\right\} + \frac{1}{r^2\theta}\frac{d\theta}{d\theta^2} + \frac{1}{X}\frac{d^2X}{d^2x} = 0 \qquad (3.20)$$

Now let

$$\frac{1}{\theta}\frac{d^2\theta}{d\theta^2} + n^2 = 0 \qquad (3.21)$$

$$\frac{1}{X}\frac{d^2X}{dx^2} + k^2 = 0$$

where n and k are arbitrary separation constants.

Then

$$\theta = A(n) \sin n\theta + B(n) \cos n\theta \tag{3.22}$$

and

$$X = C(k) \sin kx + D(k) \cos kx$$

Hence (3.20) becomes

$$\frac{d^2R}{dr^2} + \frac{1}{r}\frac{dR}{dr} - \left(k^2 + \frac{n^2}{r^2}\right) R = 0 \tag{3.23}$$

This is the modified Bessels equation which has a solution of the form

$$R = E(k)\ I_n\ (kr) + F(k)\ K_n(kr) \tag{3.24}$$

where I_n and K_n are the modified Bessel functions of the first and second kind of order n respectively. The general solution to (3.9) satisfying the condition of being finite at origin and periodic circumferentially is therefore

$$\overline{\phi} = \cos n\theta \{I_n(kr) [A(k) \cos kx + B(k) \sin kx]\} \tag{3.25}$$

Since this is a solution for any particular value of k, the most general solution will be a linear combination of all values of k.

$$\overline{\phi}(x,r,\theta) = \cos n\theta \int_0^\infty I_n(kr) [A(k) \cos kx + B(k) \sin kx]\, dk \tag{3.26}$$

The constants A, B are determined by using the boundary condition (3.14). Taking the partial derivative of equation (3.26) with respect to r and equating it to (3.14) gives:

$$\frac{\partial w}{\partial t} + U \frac{\partial w}{\partial x} = \int_0^\infty k\, I_n'(kR)\{A(k) \cos kx + B(k) \sin kx\}\, dk \cos n\theta \tag{3.27}$$

where $I_n'(kR)$ is the derivative of the modified Bessel function with respect to r.

Equation (3.27) is in a form similar to:

$$f(x) = \{\int_0^\infty \cos kx \frac{1}{\pi} \int_{-\infty}^\infty f(\xi) \cos x\xi\, d\xi + \int_0^\infty \sin kx \frac{1}{\pi} \int_{-\infty}^\infty f(\xi) \sin k\xi\, d\xi\}\, dk \tag{3.28}$$

Relation (3.28) is called the Fourier Integral theorem and represents the generalization of the Fourier expansion for an infinite interval. The quantities:

$$\frac{1}{\pi} \int_{-\infty}^\infty f(\xi) \cos k\xi\, d\xi$$
$$\frac{1}{\pi} \int_{-\infty}^\infty f(\xi) \sin k\xi\, d\xi \tag{3.29}$$

are the Fourier coefficients.

The constants A, B are then readily evaluated using (3.29). Introducing the assumed solution (3.17) the unknown constants are:

$$kI_n'(kR)A = \frac{1}{\pi} \int_0^{\ell} [(1 - \cos \frac{2p\pi x}{\ell}\, i\omega + U (\frac{2p\pi}{\ell}) \sin \frac{2p\pi x}{\ell}) \cos kx\, dx$$

cont.

$$kI_n'(kR)B = \frac{1}{\pi}\int_0^{\ell}\left[\left(1-\cos\frac{2p\pi x}{\ell}\right) i\omega + U\left(\frac{2p\pi x}{\ell}\right)\sin\frac{2p\pi x}{\ell}\right]\sin kx\,dx \tag{3.30}$$

integrating (3.30) and simplifying:

$$A = \sum_{p=1}^{\infty} \frac{1}{\pi k I_n'(kR)}\left\{\frac{(2p\pi)^2}{(2p\pi)^2-(k\ell)^2}\right\}\left\{\frac{i\omega}{k}\sin k\ell - U(\cos k\ell - 1)\right\}$$

$$B = \sum_{p=1}^{\infty} \frac{1}{\pi k I_n'(kR)}\left\{\frac{(2p\pi)^2}{(2p\pi)^2-(k\ell)^2}\right\}\left\{\frac{i\omega}{k}(1-\cos k\ell) - U\sin k\ell\right\} \tag{3.31}$$

These constants are now substituted into equation (3.26) which after considerable simplification, becomes:

$$\bar{\phi} = \sum_{p=1}^{\infty}\int_0^{\infty}\frac{I_n(kr)}{\pi k^2 I_n'(kR)}\frac{(2p\pi)^2 C_p}{[(2p\pi)^2-(k\ell)^2]}\left\{i\omega\sin k(\ell-x) + \sin kx\right\} \tag{3.32}$$

$$+ kU[\cos kx - \cos k(\ell-x)]\}\,dk\cos n\theta$$

Using now the unsteady Bernouli equation (3.8) together with the differential equation of motion for the shell, after substituting for the assumed radial displacement, result in the following equation:

$$D\left\{\left(\frac{n^4}{R^4}+\frac{1}{R^4}+\frac{2n^2}{R^4}\right)+\left[\left(\frac{2p\pi}{\ell}\right)^2+\frac{n^2}{R^4}\right]^2+\left[\frac{12(1-\nu^2)}{R^4\left(\frac{n}{R}\right)^2}\left(\frac{2p\pi}{\ell}\right)^4\right.\right.$$

$$+\frac{2(2-\nu)n^2}{R^6}\left(\frac{2p\pi}{\ell}\right)^2+\frac{n^4}{R^8}-\frac{2\nu}{R^2}\left(\frac{2p\pi}{\ell}\right)^6-\frac{6n^2}{R^4}\left(\frac{2p\pi}{\ell}\right)^4$$

$$\left.\left.-\frac{2(4-\nu)}{R^6}n^4\left(\frac{2p\pi}{\ell}\right)^2-\frac{2n^6}{R^8}\right]\frac{1}{\left[\left(\frac{2p\pi}{\ell}\right)^2+\frac{n^2}{R^2}\right]^2}\right\}\cos\frac{2p\pi x}{\ell}$$

cont.

$$-\rho m h \omega^2 \left(1 - \cos \frac{2p\pi x}{\ell}\right)$$

$$= \rho_o \sum_{p=1}^{\infty} \int_0^{\infty} \frac{I_n(kr)\, A_p}{\pi k^2 I_n'(kR)} \frac{(2p\pi)^2}{[(2p\pi)^2 - (k\ell)^2]} \tag{3.33}$$

$$\times \{(\omega^2 + k^2 U)\ (\sin k(\ell - x) + \sin kx)$$

$$+ 2k\, U\, i\omega\ (\cos k(\ell - x) - \cos kx\}\ dk$$

The method of Galerkin is now used to obtain the frequency equation, i.e., multiplying each term by $(1 - \cos \frac{2q\pi x}{\ell})$ and integrating over the length of the shell.

Non-dimensionalizing, the reference frequency is introduced:

$$\omega_o = \left(\frac{\pi}{\ell}\right)^2 \sqrt{\frac{D}{\rho_m h}} \tag{3.34}$$

and the following dimensionless variables defined:

$$\begin{aligned}
&\text{length ratio} && \lambda = \frac{\ell}{\pi R} \\
&\text{thickness ratio} && H = \frac{h}{R} \\
&\text{complex frequency} && c = \frac{\omega}{\omega_o} \\
&\text{mass ratio} && \beta = \frac{\rho_o}{\rho_m} \\
&\text{velocity} && V = U \sqrt{\frac{12(1-\nu^2)\rho_o}{\pi^2 E}} \\
&\text{integration constant} && \tau = k\ell
\end{aligned} \tag{3.35}$$

The solution thus found is:

$$[2(n^2-1)^2\lambda^4 + [2p^2+(n\lambda)^2]^2 + \frac{1}{[(2p)^2+(n\lambda)^2]^2}\frac{12(1-\nu^2)(2p)^4\lambda^4}{H^2}$$

$$+ 2(2-\nu)(2p)^2n^2\lambda^6 + n^4\lambda^8 - 2\nu(2p)^6\lambda^2 - 6n^2(2p)^4\lambda^4 \qquad (3.36)$$

$$- 2(4-\nu)(2p)^2n^4\lambda^6 - 2n^6\lambda^8\} - 3c^2] C_p \delta_{pq}$$

$$= 4\pi^4 \frac{\lambda}{H} \sum_{p=1} (2p)^2(2q)^2 \{\beta c^2 F_{1pq} + \frac{\lambda^2}{H^2} V^2 F_{2pq}\} C_p', \quad q=1,2...$$

where δ_{pq} is the Kronecker delta and F_{ipq}, i=1,2 are the improper integrals:

$$F_{1pq} = \int_0^\infty \frac{I_n(\frac{t}{\pi\lambda})}{I'_n(\frac{t}{\pi\lambda})} \frac{(1 - \cos t)}{t^3[(2p\pi)^2-t^2][(2q\pi)^2-t^2]}\, dt \qquad (3.37)$$

$$F_{2pq} = \int_0^\infty \frac{I_n(\frac{t}{\pi\lambda})}{I'_n(\frac{t}{\pi\lambda})t} \frac{(1 - \cos t)}{[(2p\pi)^2-t^2][(2q\pi)^2-t^2]}\, dt$$

These integrals are of the same form as the improper integrals given by Weaver and Unny [11], [17]. The singularities are all removable except at the lower limit t = 0, n = 0. In this case, the problem reduces to that of the uniform expansion of a bubble in a two-dimensional, incompressible flow for which this mathematical model is inadequate (see for example, Birkhoff [31] or Whitman [32]). The integrals are numerically

evaluated by using the same routine as developed by Weaver [20], which utilizes an eight point Newton-Cotes quadrature formula. The numerical values for the integrals are listed in Appendix II as a function of the circumferential mode number n and the dimensionless length ratio λ.

Equation (3.36) is an infinite set of equations and represents an eigenvalue problem in the complex frequency c with the undetermined generalized co-ordinates C_p as the eigenvector. For a non-trivial solution, the matrix of the coefficients C_p must be equal to zero.

3.4. Results and Discussion

To determine the stability behaviour of the shell, two terms of the series (3.36) were taken to give a 2 x 2 matrix, and the frequency equation found by setting the determinant of the coefficients equal to zero. The validity of using only two terms in the series to accurately represent the system will be discussed in a later paragraph. The frequency equation thus found has the simple biquadratic form

$$B_4 c^4 + B_2 c^2 + B_o = 0 \tag{3.38}$$

where

$$B_4 = \left(3 + 64\pi^4 \frac{\lambda}{H} \beta F_{111}\right) \left(3 + 1024\pi^4 \frac{\lambda}{H} \beta F_{122}\right) - \left(256\pi^4 \frac{\lambda}{H} \beta F_{112}\right)^2 \tag{3.39}$$

cont.

$$B_2 = -\left(3 + 64\pi^4 \frac{\lambda}{H} \beta F_{111}\right)\left\{2\left(n^2-1\right)^2 \lambda^4 \left[16+(n\lambda)^2\right]^2 + \right.$$

$$\frac{1}{[16+(n\lambda)^2]^2} \frac{3072\,(1-\nu^2)\lambda^4}{H^2} + 32\,(2-\nu)n^2\lambda^6 + n^4\lambda^8 - 8192\nu\lambda^2$$

$$\left. - 1536\lambda^4 n^2 - 32\,(4-\nu)n^4\lambda^6 - 2\,n^6\lambda^8 - \frac{1024\pi^4\lambda^3 F_{222} V^2}{H^3}\right\}^{\prime}$$

$$-\left\{2(n^2-1)^2\lambda^4 + [4+(n\lambda)^2]^2 + \frac{1}{[4+(n\lambda)^2]^2} \frac{192\,(1-\nu^2)\lambda^4}{H^2}\right.$$

$$+ 8(2-\nu)n^2\lambda^6 + n^4\lambda^8 - 128\nu\lambda^2 - 96n^2\lambda^4 - 8(4-\nu)n^4\lambda^6$$

$$\left. - 2n^6\lambda^8 - \frac{64\pi^4\lambda^3 F_{211} V^2}{H^3}\right\}^{\prime\prime} \times \left(3 + 1024\pi^4 \frac{\lambda}{H} \beta F_{122}\right)$$

$$-\left(512\pi^4 \frac{\lambda}{H} \beta F_{112}\right)\left(256\pi^4 \frac{\lambda^3}{H^3} F_{212} V^2\right)$$

$$B_0 = \left\{\quad\right\}^{\prime} \times \left\{\quad\right\}^{\prime\prime} - \left(256\pi^4 \frac{\lambda^3}{H^3} F_{112} V^2\right)^2$$

This equation is solved exactly for the frequency c, over a wide range of flow velocity V, assuming various values for the parameters λ, H and n. Real c gives the frequency of oscillation while negative imaginary c represents non-oscillatory divergence instability.

Typical results for the frequency of the first

mode as a function of flow velocity is shown in Figures 3.2 and 3.3. The frequency gradually decreases with increasing flow velocity until it finally becomes zero, where static divergence occurs. This is similar to that discussed in reference [11] for pin-ended shells, and the corresponding variation of the frequency as a function of flow velocity is also shown in these figures. For the shell $\frac{\ell}{R} = 45$ and $\frac{h}{R} = 0.02$ in Figure 3.2 the instability is lost in the beam mode, i.e., $n = 1$, $p = 1$. However depending on the length and thickness ratios, the stability is generally lost in a mode corresponding to some number of circumferential waves greater than one, $n>1$. For the shell $\frac{\ell}{R} = 5$ and $\frac{h}{R} = 0.02$ in Figure 3.3 the "critical mode" is $n = 3$, $p = 1$. To ascertain the effect of circumferential mode number, n, on the divergence velocity, numerous calculations were made. A typical result is shown in Figure 3.4. Clearly the divergence velocity is quite sensitive to n. For this shell, $\frac{\ell}{R} = 10$ and $\frac{h}{R} = 0.02$, the lowest velocity at which instability occurs corresponds to the mode shape $p = 1$, $n = 2$, which is the critical mode shape for this particular shell. This minimum flow velocity is the one of interest and is called the critical divergence velocity V_C. Generally the number of circumferential waves associated with the critical divergence velocity increases for decreasing thickness ratio and/or length ratio.

To obtain a better understanding of the mode shape associated with the critical divergence velocity, a comparison

was made with the mode shape of the lowest natural frequency at zero flow velocity. Numerous calculations of the divergence velocity V and the natural frequency c as a function of the circumferential mode number n were carried out. Typical results for a specific thickness ratio but various length ratios are shown in Figure 3.5 and Figure 3.6. Figure 3.6 shows that the minimum, or fundamental, frequency for the shells with length ratios of 45, 10 and 5 is associated with 1, 2 and 3 circumferential waves respectively. Clearly, the minimum, or critical, divergence velocity for each of these shells co-responds to the same mode shape.

That this is true is not really surprising when the strain energy in the shell during deformation is considered. The stretching energy is strongly dependent on the number of axial half-waves while the bending energy depends largely on the number of circumferential waves as demonstrated schematically in Figure 3.7. The mode shape corresponding to the minimum total strain energy for any particular shell will then be the one requiring the minimum flow velocity for instability, i.e., the critical flow velocity of that shell.

This mode shape is also that corresponding to the lowest natural frequency of the shell. In addition, for a given number of circumferential waves, the natural frequency increases monotonically as the number of axial half-waves increases. (This is not generally true for an increase in the number of circumferential waves). Therefore the critical mode shape for divergence will always have one axial half-wave

p = 1 and a number of circumferential waves depending on the length and thickness ratios. Only relatively long shells will have a critical mode shape corresponding to an Euler column p = 1, n = 1.

The convergence of the solution was investigated by taking one, two and three terms of the infinite series (3.36) and typical results are shown in Figure 3.8. It is seen that additional terms do not improve the solution for the beam mode n = 1, p = 1. However when a number of circumferential waves are considered, more than one term is necessary. Apparently for higher numbers of circumferential waves, more terms are required depending on the length ratio. However, it appears, at least for the range of parameters studied here, that two terms are sufficient for determining the critical stability boundary.

The minimum flow velocity to give divergence instability regardless of the number of circumferential waves have been plotted in Figure 3.9 for various values of length ratios. Clearly for shorter and thinner shells, the critical flow velocities are associated with higher number of circumferential waves. Furthermore for thicker and longer shells the lower are the number of circumferential waves associated with the critical flow velocities until n = 1 which is the simple beam mode.

3.4.1. Limiting Case of a Long Shell

In reference [11] the general theory for a pin-ended shell is considered in the limiting case of a long shell where

the beam mode is the critical mode shape (n=1). As was discussed in reference [11] and has been seen in Figure 3.9, for relatively large length ratios the critical mode is the beam mode. The critical divergence velocity for a pin-ended shell in the limiting case is

$$U_{pin} = \frac{\pi}{\ell}\sqrt{\frac{EI}{m}} \tag{3.40}$$

It is of interest to consider the same limiting case for the present theory. At the divergence boundary the natural frequency of the shell is zero and the desired velocity may be found by considering B_o in equation (3.32). For the first beam mode this reduces to

$$\left\{ \quad \right\}'' = 0 \tag{3.41}$$

Assuming that

$\lambda >> 1$ and $n = 1$, equation (3.41) becomes

$$V^2 = \frac{12\,(1-\nu^2)\,H}{4\pi^4\,\lambda^3\,F_{211}} \tag{3.42}$$

Then using the definition for the various parameters (3.35) and introducing the moment of inertia for a thin cylinder

$$I = \pi R^3 h \tag{3.43}$$

and mass of fluid per unit length of shell

$$m = \pi R^2 \rho \tag{3.44}$$

equation (3.42) becomes

$$U = \frac{1}{4\pi\sqrt{\lambda\ F_{211}}} \times \frac{2\pi}{\ell} \sqrt{\frac{EI}{m}} \tag{3.45}$$

This expression for the critical divergence velocity, is twice that for a pin-ended shell except for the term $\frac{1}{4\pi\sqrt{\lambda\ F_{211}}}$. Since the effective length for a clamped-ended column is $\frac{\ell}{2}$ it is reasonable to expect in view of equation (3.40) that

$$U_{clamp} = \frac{2\pi}{\ell} \sqrt{\frac{EI}{m}} \tag{3.46}$$

The first term in equation (3.45) is called the "end flow factor" [11] and arises from the particular assumption made in the present analysis regarding the flow condition at the ends of the shell. As such it is expected to become negligible for longer shells. In Figure 3.10 this factor is plotted versus $\frac{\ell}{R}$. It is interesting to see that for a length ratio of $\frac{\ell}{R} = 16$ the effect on the divergence velocity is less than one percent.

Figure 4.2 compares plots of the full theory and the approximation given by equation (3.46). It is seen that for this particular shell the approximate solution is indistinguishable from the full solution for shells longer than about fifteen-

diameters. For shells about ten diameters long the beam approximation predicts a divergence velocity about 7% high.

Note that this simple solution will only give the correct divergence velocity as long as the critical mode is the beam mode n = 1. For very thin shells, the critical mode may be associated with n > 1, even for relatively long shells as shown in Figure 3.9. In such cases, even though the correct velocity may be predicted for instability in the n = 1 mode, the critical flow velocity will generally be much lower. An example can be taken from Figure 3.8 where the divergence velocity for $\frac{\ell}{R} = 20$ and n = 1 is about 0.04 whereas the critical divergence velocity occurs for n = 2 at about $V_{Cr} = 0.025$.

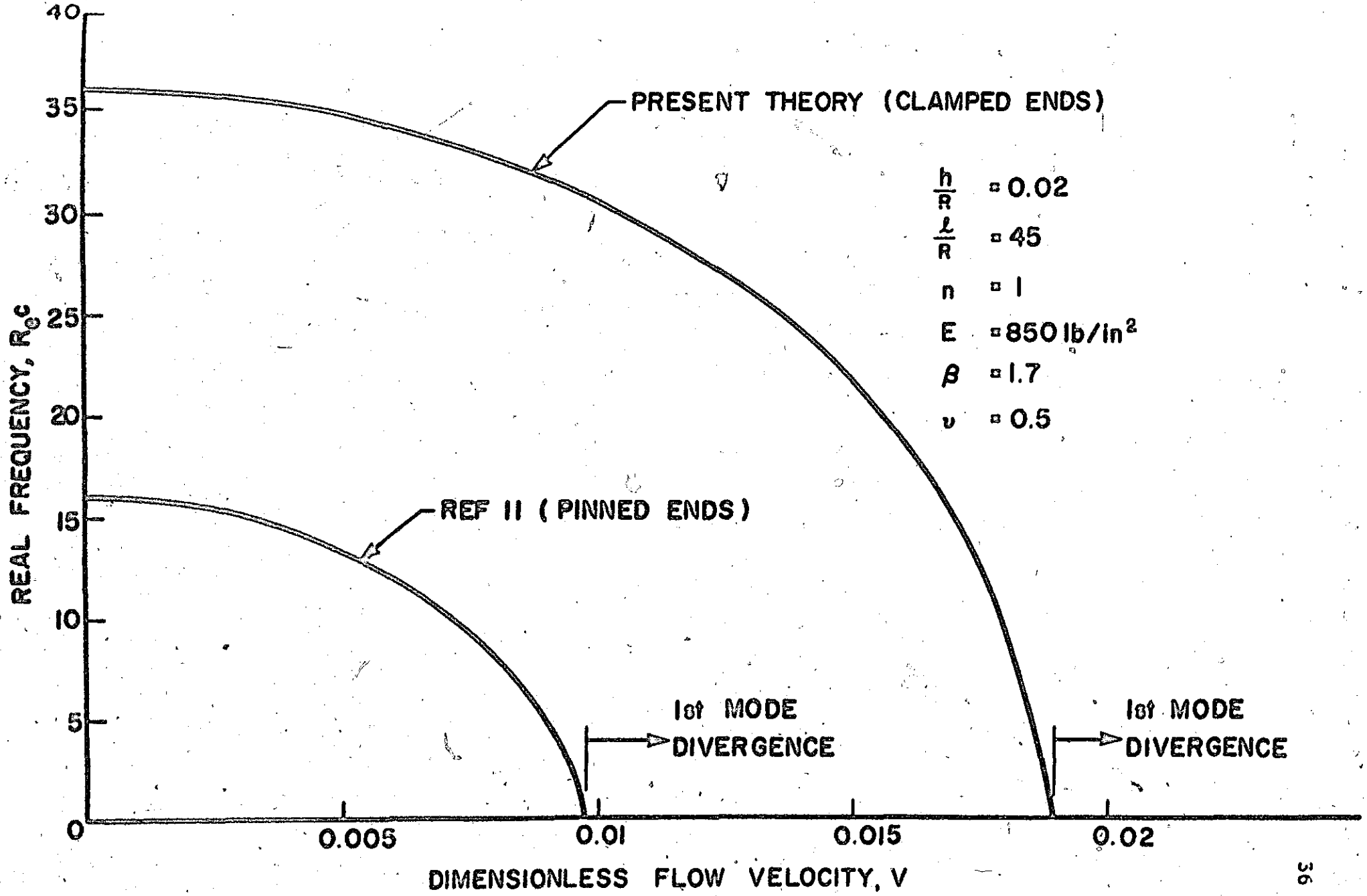
PRESENT THEORY (CLAMPED ENDS)
REF 11 (PINNED ENDS)
h/R = 0.02
ℓ/R = 45
n = 1
E = 850 lb/in²
β = 1.7
υ = 0.5
1st MODE DIVERGENCE
1st MODE DIVERGENCE
REAL FREQUENCY, R_ω^c
DIMENSIONLESS FLOW VELOCITY, V
0
5
10
15
20
25
30
35
40
0.005
0.01
0.015
0.02

FIG. 3.2

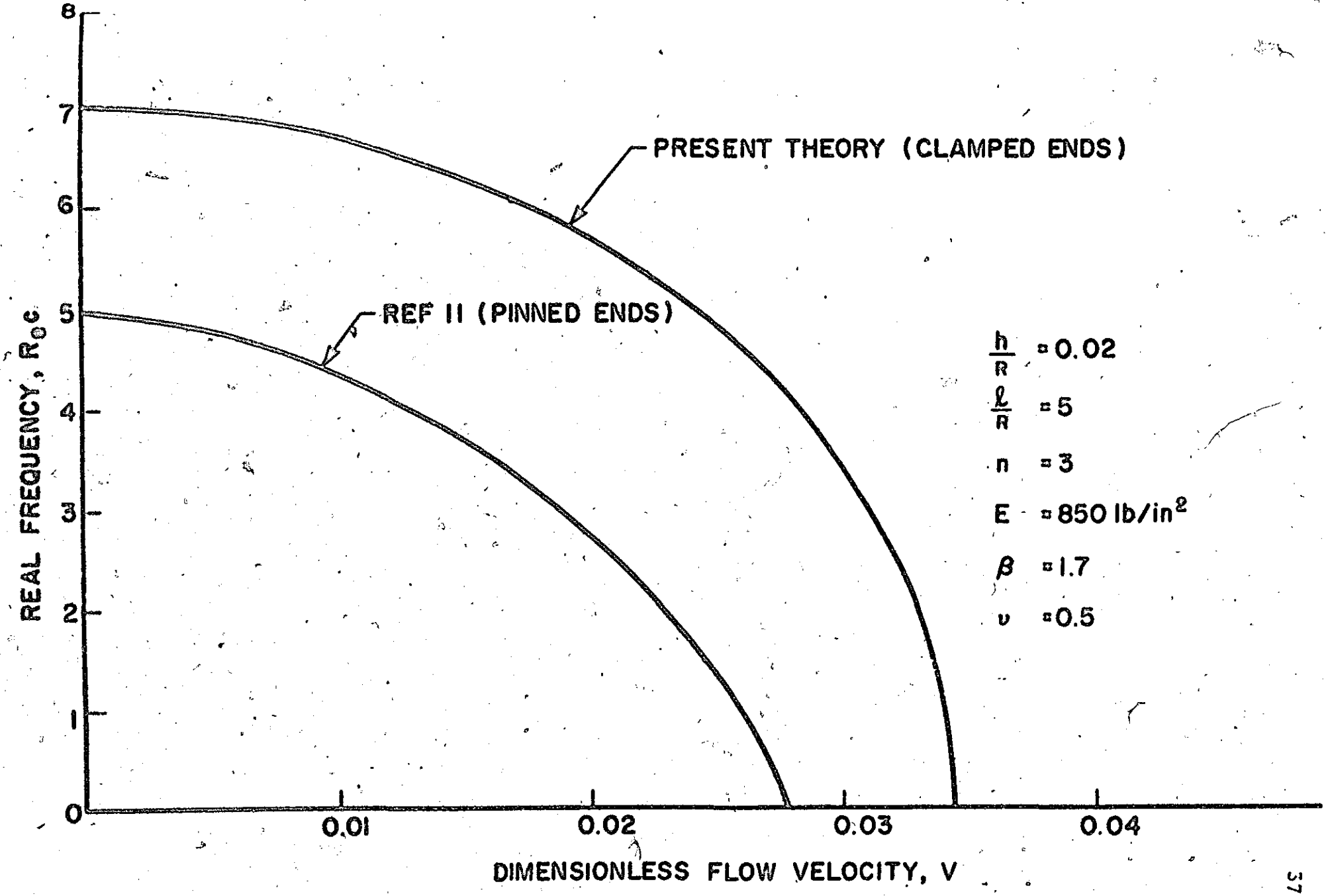
PRESENT THEORY (CLAMPED ENDS)
REF 11 (PINNED ENDS)
h/R = 0.02
ℓ/R = 5
n = 3
E = 850 lb/in²
β = 1.7
ν = 0.5
REAL FREQUENCY, R₀c
DIMENSIONLESS FLOW VELOCITY, V
0
1
2
3
4
5
6
7
8
0.01
0.02
0.03
0.04

FIG. 3.3

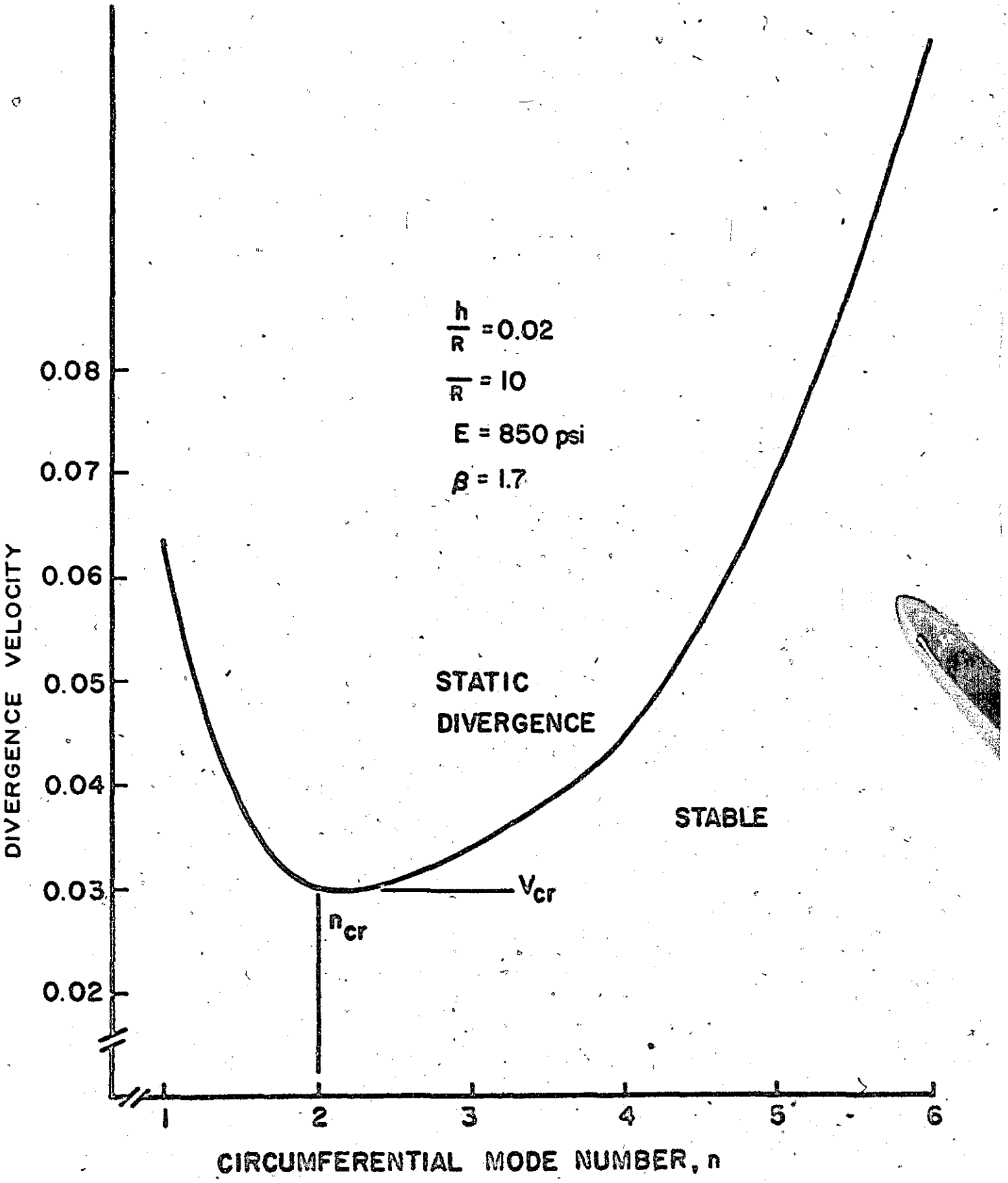
$\frac{h}{R}$ = 0.02
$\frac{}{R}$ = 10
E = 850 psi
β = 1.7
STATIC
DIVERGENCE
STABLE
V_{cr}
n_{cr}
DIVERGENCE VELOCITY
0.08
0.07
0.06
0.05
0.04
0.03
0.02
1
2
3
4
5
6
CIRCUMFERENTIAL MODE NUMBER, n

FIG. 3.4

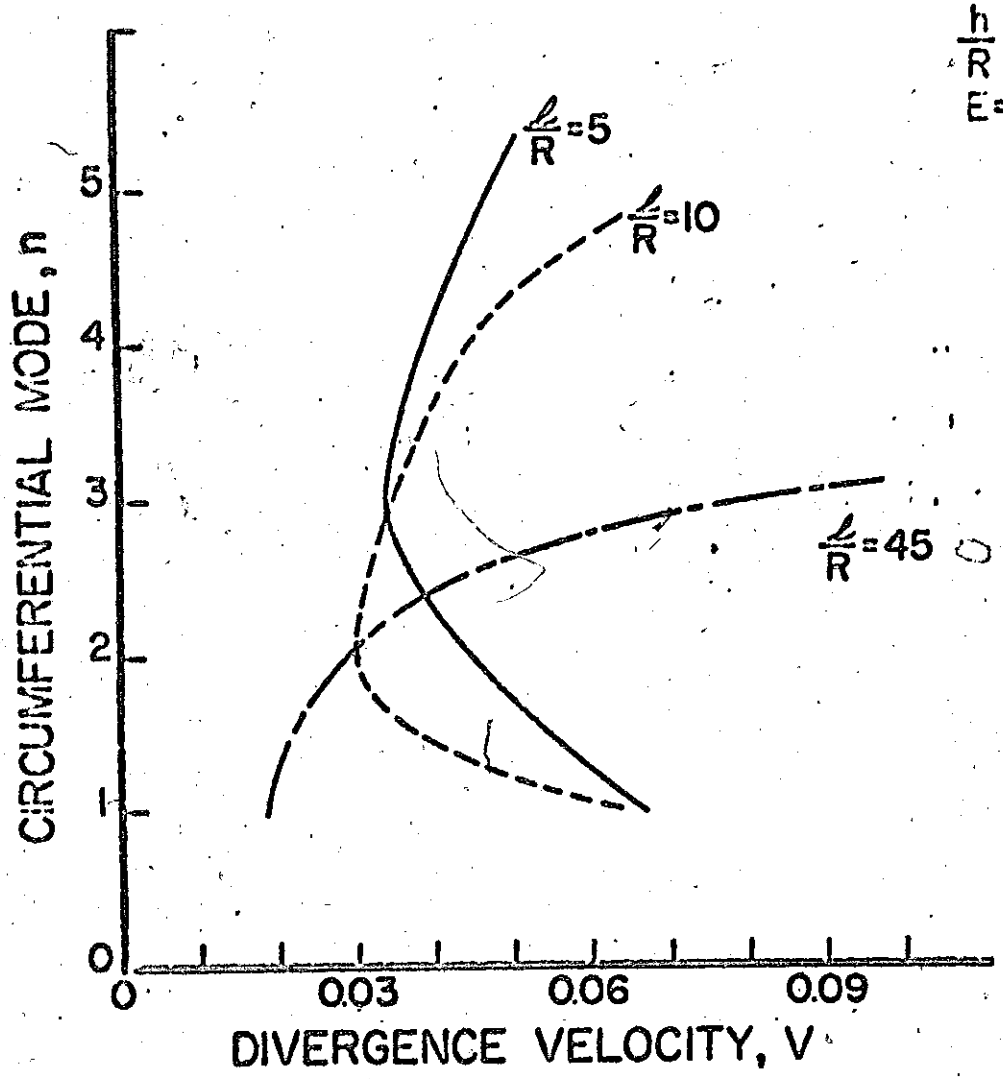
CIRCUMFERENTIAL MODE, n
0
1
2
3
4
5
$\frac{\ell}{R}$=5
$\frac{\ell}{R}$=10
$\frac{\ell}{R}$=45
0
0.03
0.06
0.09
DIVERGENCE VELOCITY, V

FIG 3.5

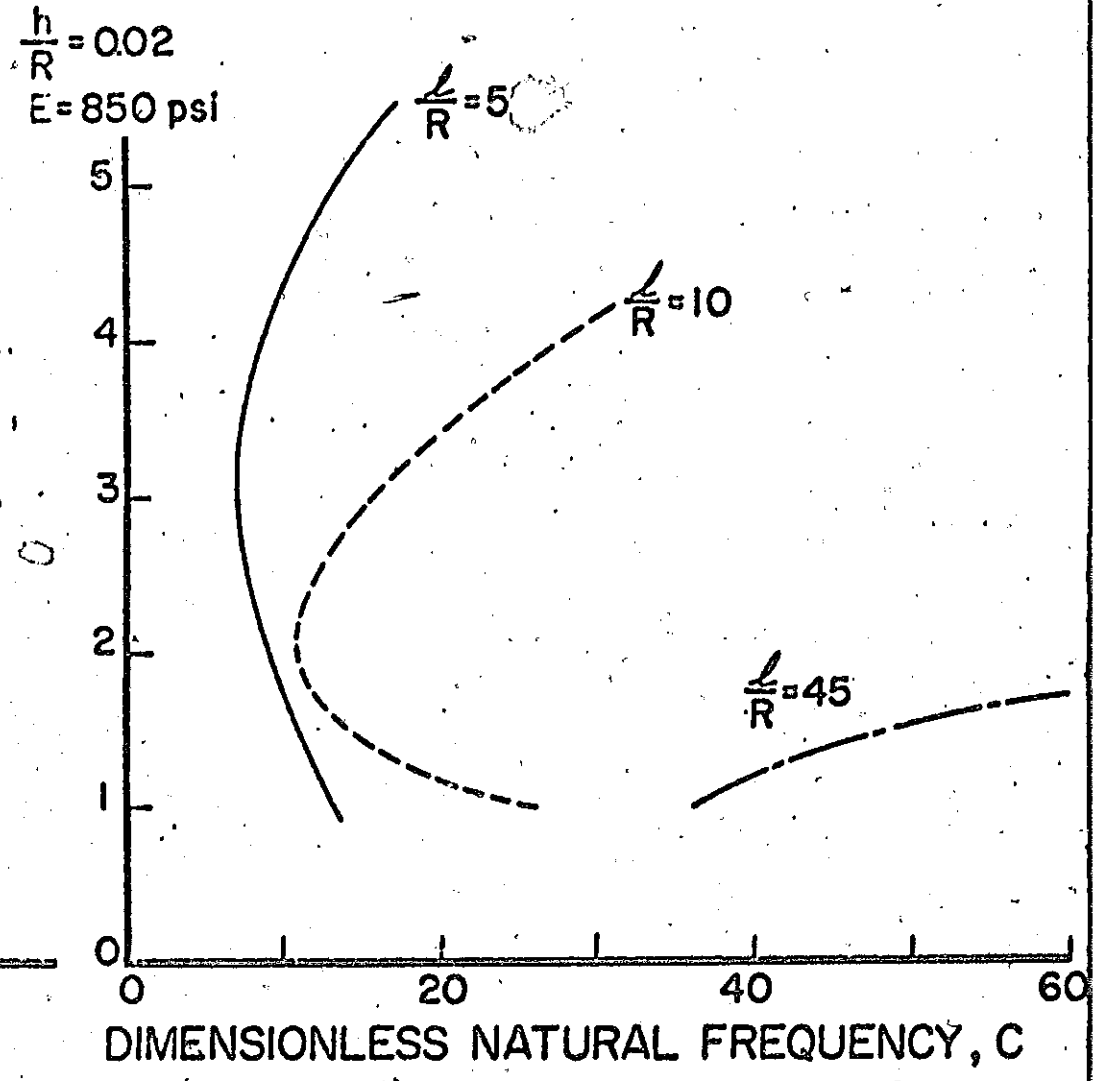
$\frac{h}{R}$=0.02
E=850 psi
0
1
2
3
4
5
$\frac{\ell}{R}$=5
$\frac{\ell}{R}$=10
$\frac{\ell}{R}$=45
0
20
40
60
DIMENSIONLESS NATURAL FREQUENCY, C

FIG 3.6

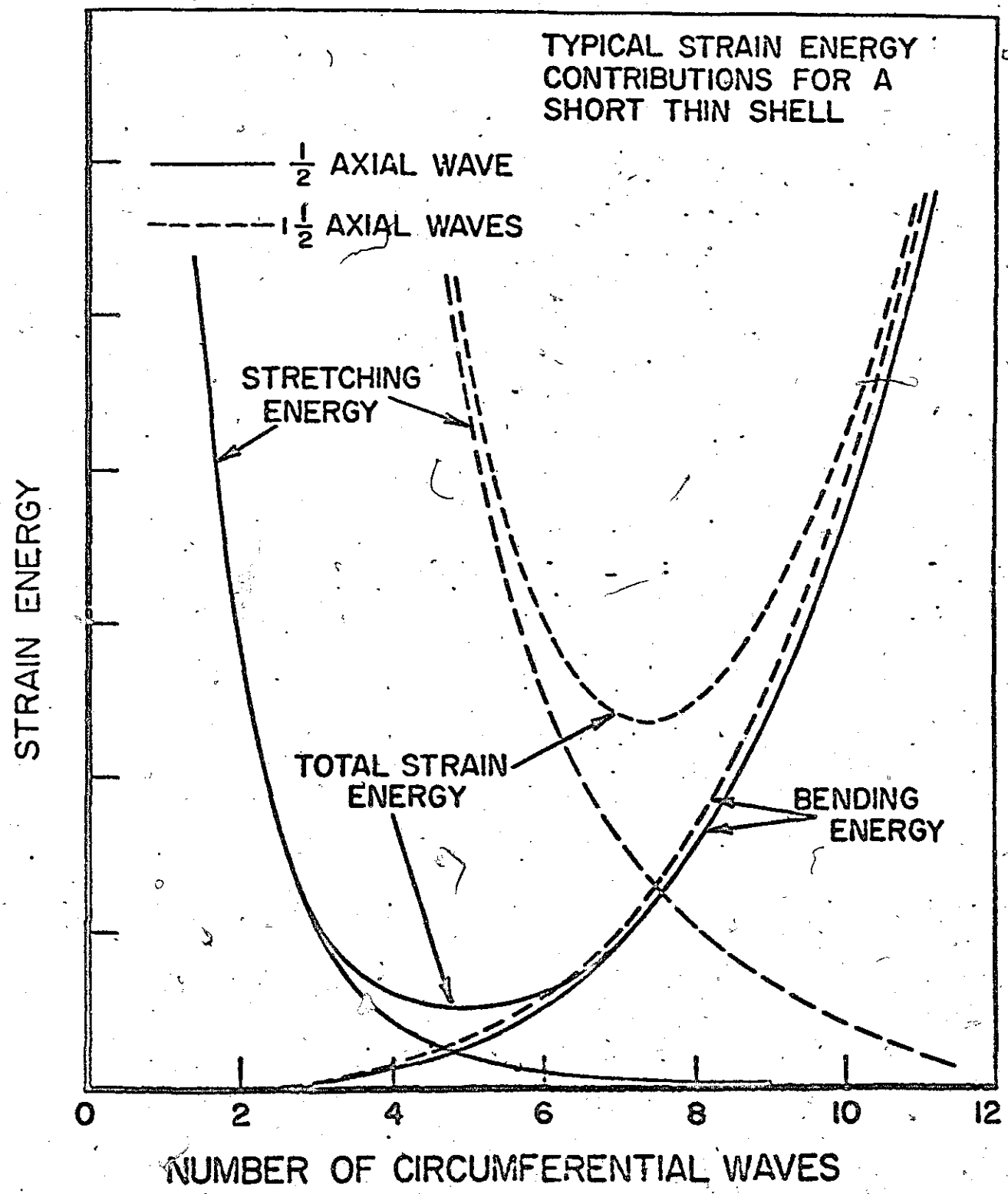
TYPICAL STRAIN ENERGY CONTRIBUTIONS FOR A SHORT THIN SHELL
½ AXIAL WAVE
1½ AXIAL WAVES
STRETCHING ENERGY
TOTAL STRAIN ENERGY
BENDING ENERGY
STRAIN ENERGY
0
2
4
6
8
10
12
NUMBER OF CIRCUMFERENTIAL WAVES

FIG 3.7

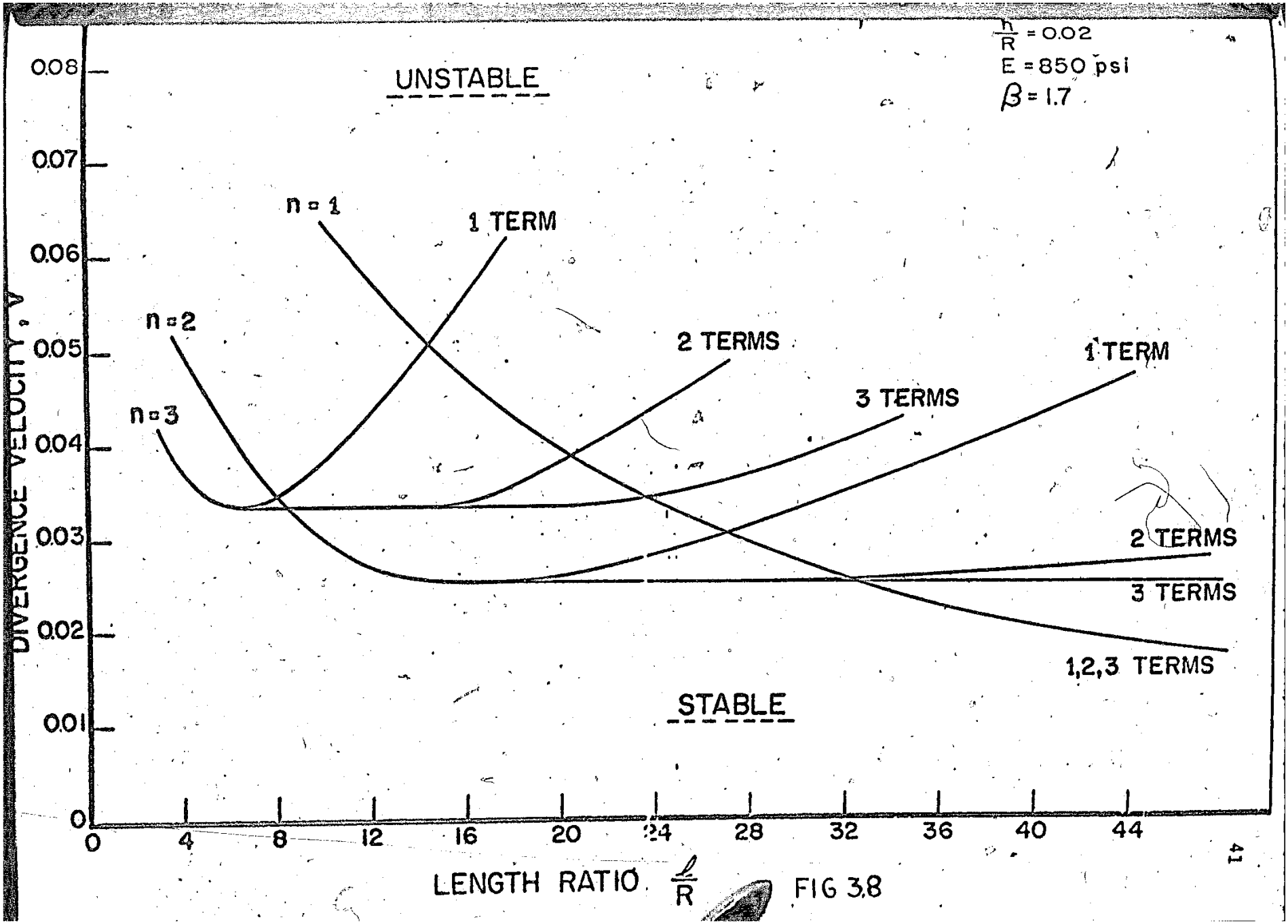
h/R = 0.02
E = 850 psi
β = 1.7
UNSTABLE
STABLE
n = 1
1 TERM
n = 2
2 TERMS
n = 3
3 TERMS
1 TERM
2 TERMS
3 TERMS
1,2,3 TERMS
DIVERGENCE VELOCITY, V
0.08
0.07
0.06
0.05
0.04
0.03
0.02
0.01
0
0
4
8
12
16
20
24
28
32
36
40
44
LENGTH RATIO l/R

FIG 3.8

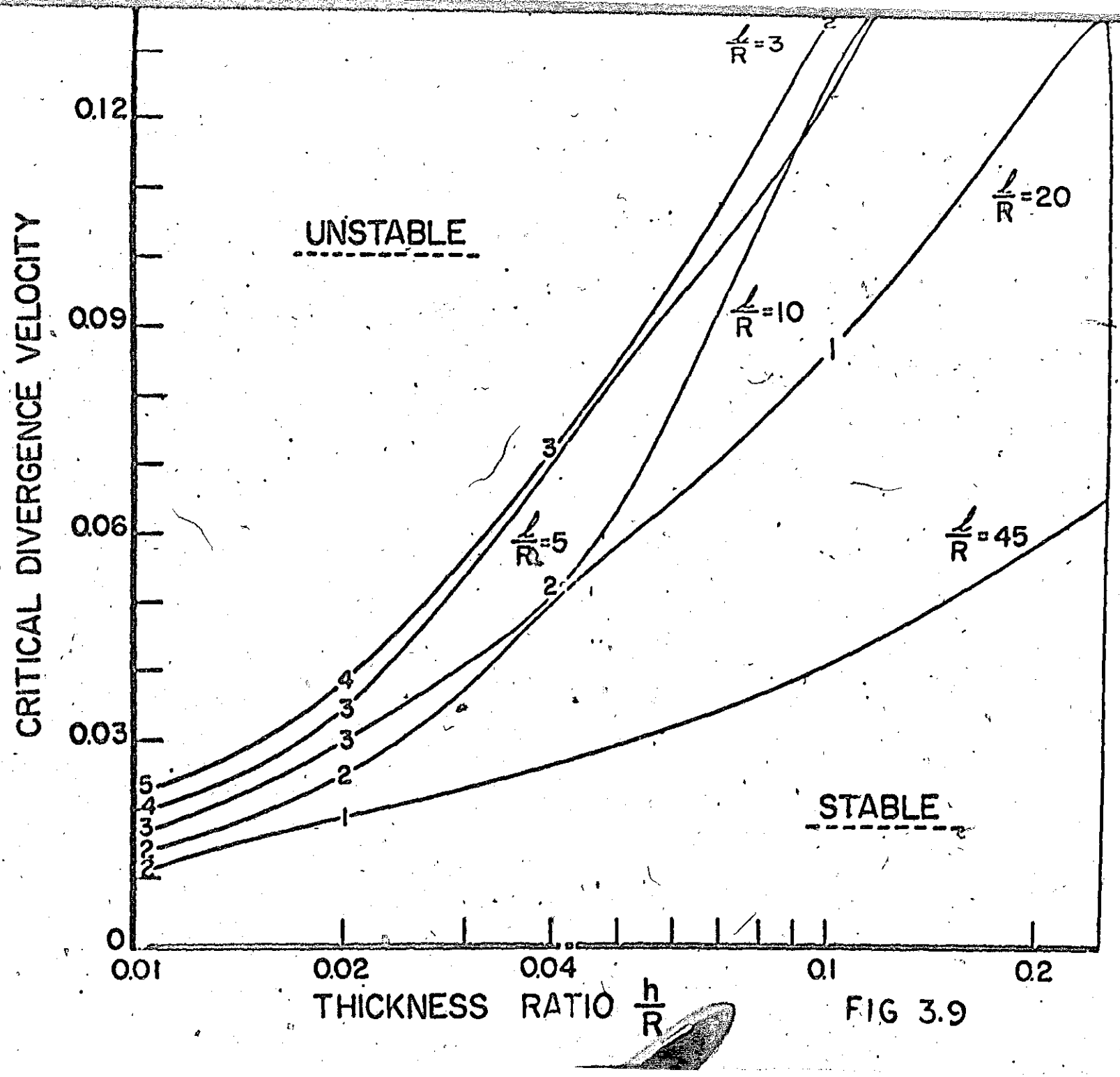
CRITICAL DIVERGENCE VELOCITY
0.12
0.09
0.06
0.03
0
UNSTABLE
STABLE
$\frac{l}{R}=3$
$\frac{l}{R}=10$
$\frac{l}{R}=20$
$\frac{l}{R}=5$
$\frac{l}{R}=45$
5
4
3
2
1
0.01
0.02
0.04
0.1
0.2
THICKNESS RATIO $\frac{h}{R}$

FIG 3.9

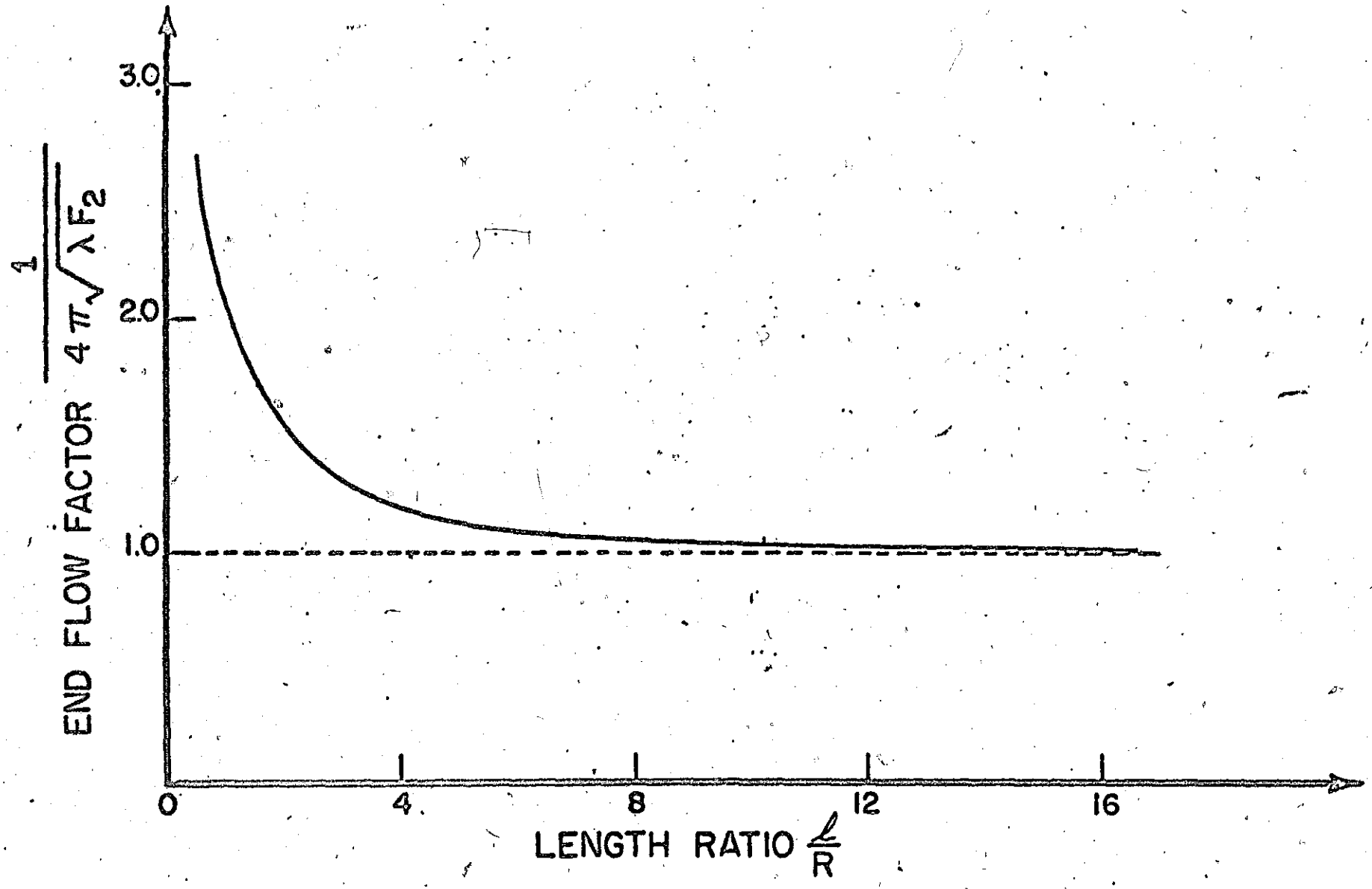
END FLOW FACTOR $\frac{1}{4\pi\sqrt{\lambda F_2}}$
3.0
2.0
1.0
0
4
8
12
16
LENGTH RATIO $\frac{\ell}{R}$

FIG 3.10

CHAPTER 4

EXPERIMENTAL ANALYSIS

4.1. General

The aim of the experiments was to confirm the validity of the theoretical results obtained above, concerning the stability associated with a clamped-ended tube conveying fluid, and to observe the different instability phenomena, possible for a cylindrical shell. These are divergence in the beam mode, circumferential divergence and "flutter", although the latter was not predicted by the theory given above. Unfortunately the only quantitative results obtained which are considered to be reliable are of the beam mode instability.

4.2. Description of the Experimental Apparatus

Figure 4.1 shows diagrammatically the apparatus used in the experiments with tubes conveying water. The tubes were fitted over aluminum adaptors with the external diameter slightly larger than the internal diameter of the tube. The inlet adaptor was made one foot long to act as a flow straightner. This adaptor was screwed onto the pipe supplying the water and the pipe itself was securely attached to a metal frame, so that the whole structure was quite rigid. The outlet adaptor was fitted into a linear ball bearing to ensure that no axial stresses were set up in the tube, either when setting up the experiment, or when the tube became unstable. By this arrangement

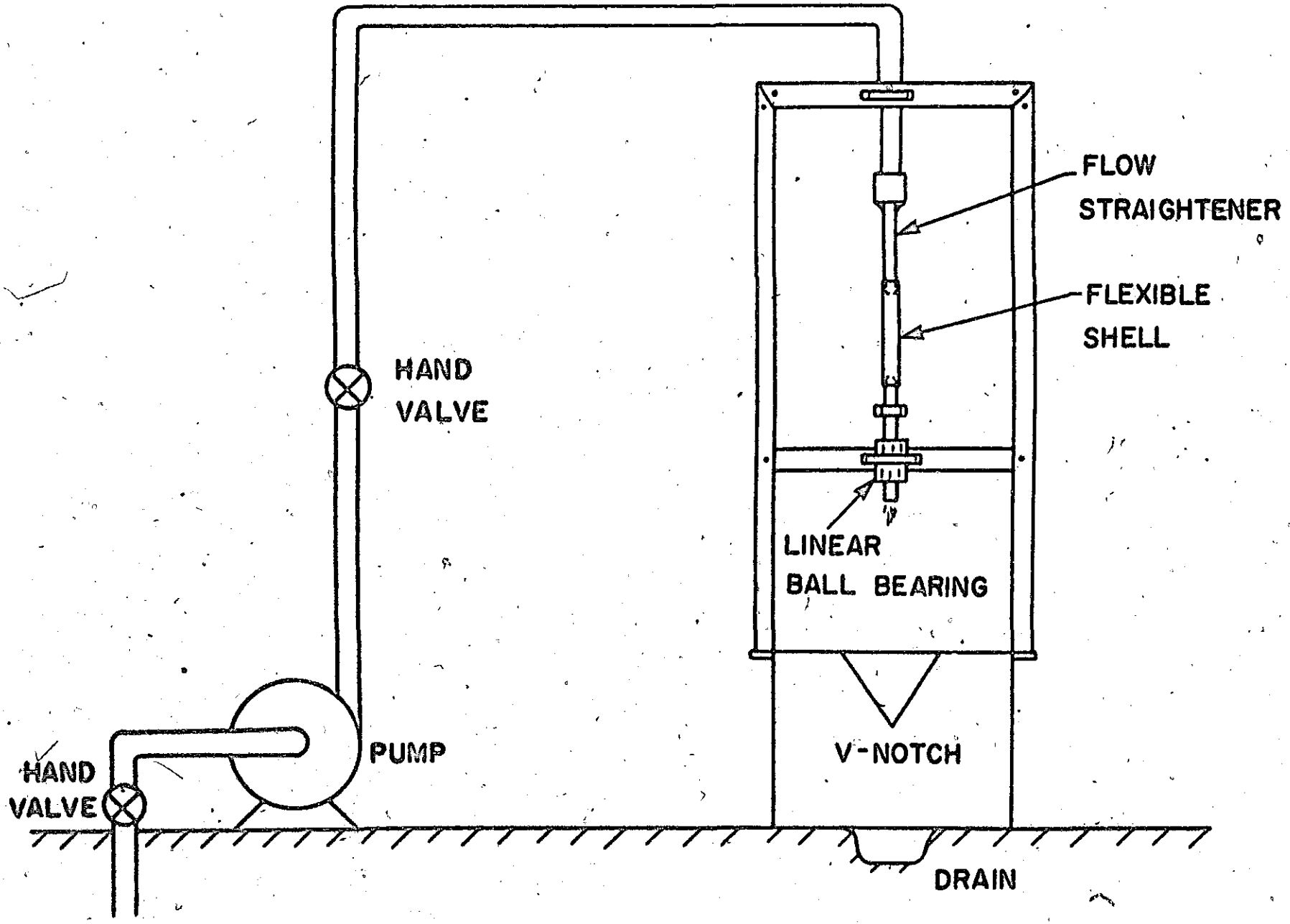
FLOW
STRAIGHTENER
FLEXIBLE
SHELL
HAND
VALVE
LINEAR
BALL BEARING
PUMP
HAND
VALVE
V-NOTCH
DRAIN

FIG. 4.1

the boundary condition was identical to the one used in the theory.

A centrifugal pump capable of delivering 100 IGPM at a head of 240 feet was used to supply the water. Flow velocities up to 50 ft./sec. were therefore available in the one inch diameter tube. The water, after leaving the outlet adaptor, was collected in a tank with a v-notch fitted to measure the volume flow. The water flow was controlled by a manually operated valve in the supply line. The flow velocity in the tube was calculated by dividing the volume flow by the area of the tube. The tubes used were either latex rubber or commercially available Tygon tubing. The latex tubes were specially made for this experiment by using a dipping method. A one inch diameter steel rod was emerged into a liquid latex bath and quickly withdrawn. This method allowed only one dipping and the resulting tube had a wall thickness of only 0.010 inches. By using a coagulant a second dipping could be performed but this resulted in a varying wall thickness. The experiments conducted with these thin latex tubes were extremely difficult as they had a tendency to burst or go into a violent fluttering at the lower end. None of those experiments gave any reliable quantitative results, therefore the results reported here were obtained by using the Tygon tubes.

The observation of the dynamic behaviour of the tube with increasing flow velocity was made visually.

4.3. Correlation between Theory and Experiments

The critical flow velocity V_c was obtained by increasing the fluid velocity in small steps, allowing sufficient time at each step for a steady state condition to be achieved and the new flow velocity to be read until instability occurred where the measurement of V_c was made. The behaviour of the tube at each step was assessed by giving the tube a small push and observing the resulting motion. For increasing flow the natural frequency of the tube was observed to decrease until becoming zero. At that point the tube buckled similar to the buckling of a column and the tube had to be supported laterally. At slightly higher velocities flutter occurred. The flutter mode seemed to be a simple flattening of the tube in one direction. The same flapping can be produced by pinching the tube at flow velocities somewhat below the critical. It appears that the theoretical predicted flutter modes [10], [11] are not those observed experimentally and that the latter may be an entirely different phenomenon.

These experiments were repeated for various length ratios between $\ell/R = 12.8$ and $\ell/R = 43$. Shorter tubes were not tested due to the extremely high divergence velocities for these tubes, which makes the experiment hazardous. For a length ratio of $\ell/R = 12.8$ the divergence velocity was found to be 45.6 ft./sec.

The experimental values for the dimensionless critical flow velocity are compared in Figure 4.2 with the

theoretical values for different length ratios. As seen from Figure 4.2, the results are quite reasonable, the agreement being within 10%. It is felt that the discrepancy between theory and experiments is due to the excessive thickness ratio of the tubes tested and that for the beam mode and thickness ratios less than about 0.1, the theory will give very accurate predictions. Note that for this particular tube the beam approximation seems to deteriorate for tubes less than about ten diameters long.

4.4. Comparison with Previous Work

As there already existed theoretical and experimental results for a clamped-ended tube conveying fluid [10] it was considered desirable to compare the present predictions with these results. Calculations were then performed for the tube considered in reference [10] using the present theory as well as the theory for pinned-ended tubes of reference [11]. The results are shown in Figure 4.3.

For long tubes $\ell/R > 38$ the predictions of the present theory are identical with those of reference [10], i.e., when the instability is lost in the beam mode $p = 1$, $n = 1$. For shorter tubes, when the instability is lost in circumferential modes greater than one, the present theory gives higher critical flow velocities than those given by Paidoussis and Denise, although the difference is quite small for some length ratios. It is interesting to note that the deviation between

the two theories is highest at length ratios where a change in the critical circumferential mode occurs. The difference may be attributed to the fact that in reference [10] the full Flugge equations are used, and to the different flow conditions assumed at the ends of the tube in the two theories. These are shown schematically in Figure 4.4. As the full Flugge equation is used in reference [10], one would expect better results compared with the present theory on that account. However, as shown in Figure 4.4 the boundary condition assumed at the ends of the tube in the present theory, more closely resembles the actual case. Another advantage of the present theory is its relative simplicity.

As expected the pinned-ended solution represents a lower bound on the experimental results and can be used as a conservative estimate of the critical flow velocity. Note also that as shown in Figures 3.2 and 3.3 the difference between the pinned-ended solution and the clamped-ended, decreases for shorter shells.

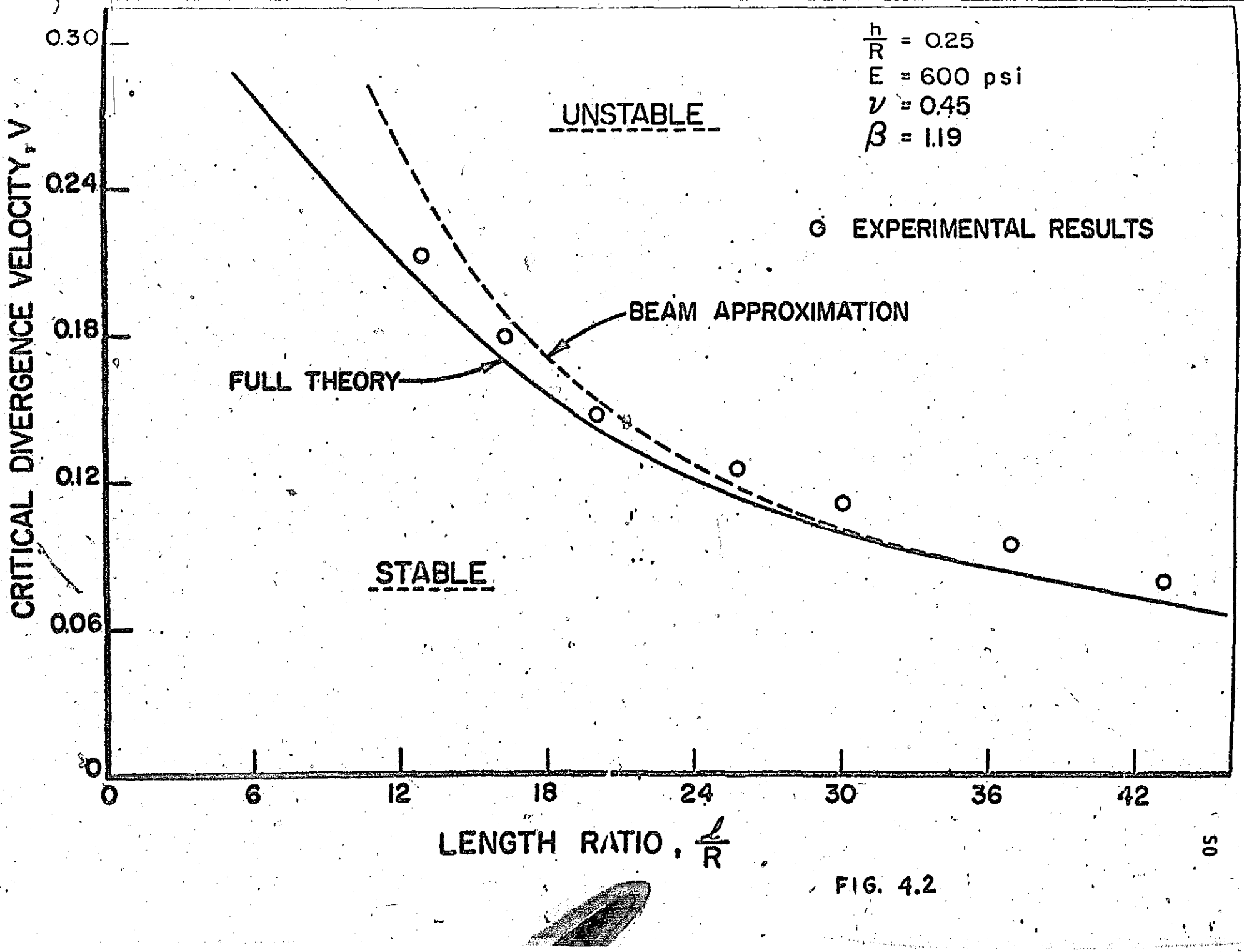
$\frac{h}{R}$ = 0.25
E = 600 psi
ν = 0.45
β = 1.19
UNSTABLE
STABLE
EXPERIMENTAL RESULTS
BEAM APPROXIMATION
FULL THEORY
CRITICAL DIVERGENCE VELOCITY, V
0.30
0.24
0.18
0.12
0.06
0
0
6
12
18
24
30
36
42
LENGTH RATIO, $\frac{\ell}{R}$

FIG. 4.2

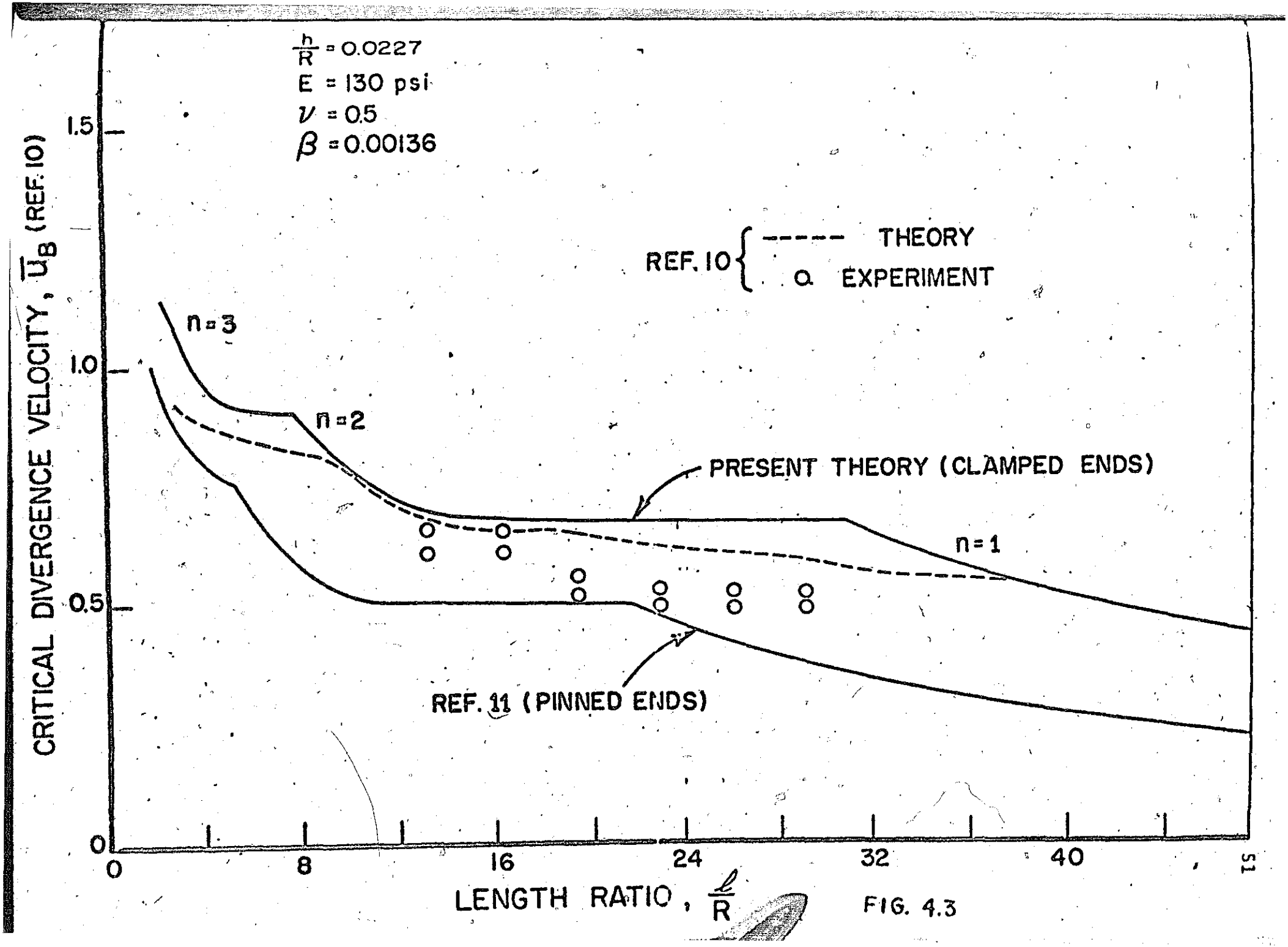
$\frac{h}{R}$ = 0.0227
E = 130 psi
ν = 0.5
β = 0.00136
REF. 10 { ----- THEORY
o EXPERIMENT
n = 3
n = 2
n = 1
PRESENT THEORY (CLAMPED ENDS)
REF. 11 (PINNED ENDS)
CRITICAL DIVERGENCE VELOCITY, $\bar{U}_B$ (REF. 10)
LENGTH RATIO, $\frac{\ell}{R}$
0
0.5
1.0
1.5
8
16
24
32
40
51

FIG. 4.3

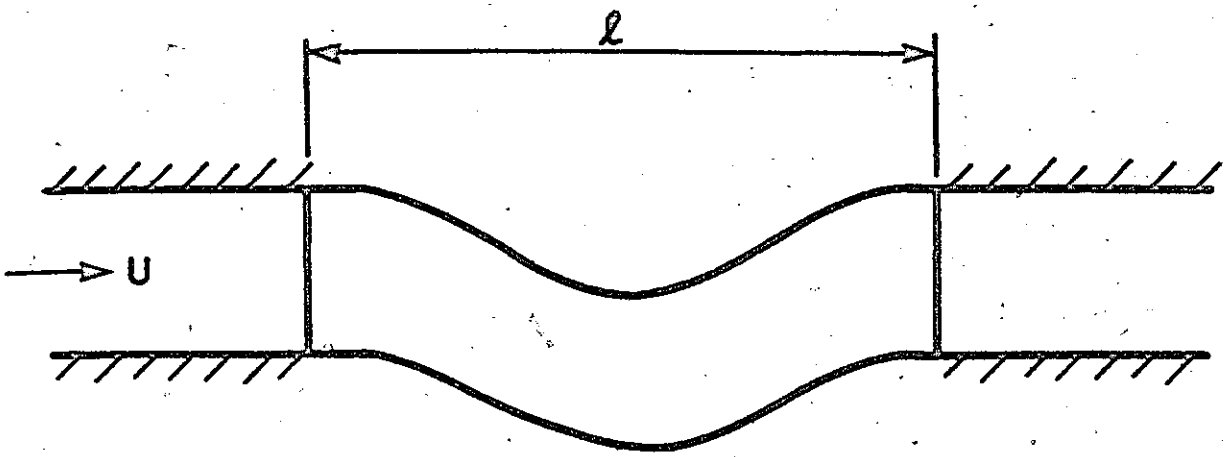

END CONDITIONS
OF PRESENT THEORY

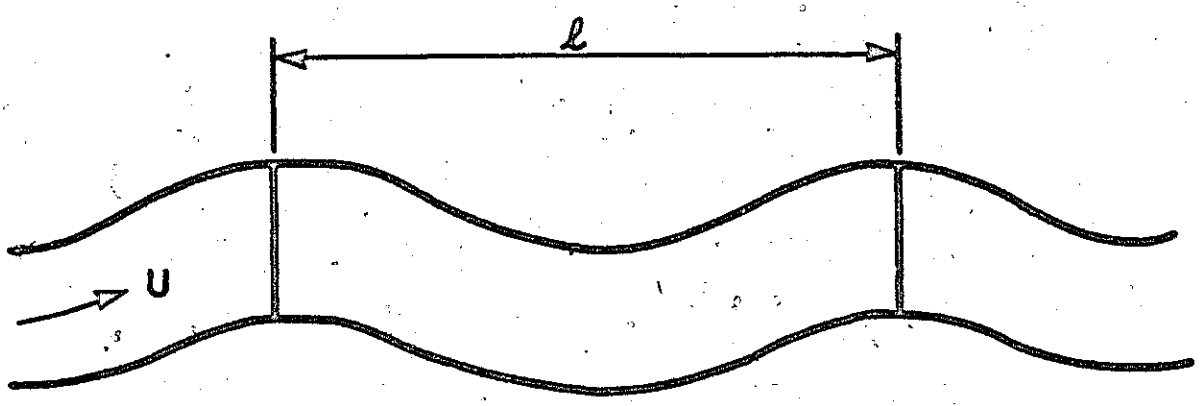

END CONDITIONS
OF REFERENCE [10]

FIG. 4.4

CHAPTER 5

CONCLUSION AND RECOMMENDATIONS

The theory used by Unny and Weaver [11] has been extended to determine the stability behaviour of clamped-ended shells conveying internal incompressible flow. Such a shell is found to become unstable through static divergence while flutter occurs for higher flow velocities. Depending on the thickness and length ratios of the shell, the mode of instability is a combination of the beam mode $p = 1$, and a number of circumferential waves. The shorter and thinner the shell the higher the number of circumferential waves. For sufficiently long shells the critical mode is the beam mode $p = 1$, $n = 1$ and a very simple analytical expression may be used to accurately predict the critical divergence velocity. The mode shape at the critical divergence velocity is the same as that corresponding to the fundamental frequency of the shell.

The theoretical results have been compared with experiments as well as with previous theoretical and experimental work and the agreement was found to be reasonably good. In connection with the last point it is noted that the measured critical divergence velocities are higher than the theoretical ones. One reason for this as given in section 4.4, could be the extensive thickness ratio of the tubes tested. It is expected that for thickness ratios below 0.1 the theory will

give quite accurate results. This should be confirmed by new experiments. When the theoretical results are compared with the results of reference [10] they give higher values for the critical divergence velocities. In reference [10] the full Flugge equation of motion for a shell is used and on that account one would expect the theory to give better results. However, the boundary conditions assumed in the present theory more closely resembles the actual case. The experimental values given by reference [10] are on the low side of the theoretical results, while our experiments give higher values than predicted by the theory. It is therefore difficult to judge which theory is the most accurate.

The present analysis has the unfortunate characteristic that it cannot predict "flutter". This is due to the assumed solution which contains only odd axial modes. As flutter is produced by coupling of odd and even modes it cannot be predicted by the present solution. The theory can be refined to include these instabilities by assuming a solution that contains odd and even modes. A suitable solution would be:

$$\sum_{p} \left\{ \cos \frac{(p-1)\pi x}{\ell} - \cos \frac{(p+1)\pi x}{\ell} \right\} \qquad (5.1)$$

REFERENCES

1. H. Ashley and G. Haviland, 1950 Journal of Applied Mechanics 17, 229-232. Bending vibrations of a pipe-line containing a flowing fluid.

2. E. I. N. Niordson, 1953 Transactions of the Royal Institute of Technology, Stockholm, 73. Vibration of a cylindrical tube containing flowing fluid.

3. H. L. Dodds, Jr, and H. L. Runyan, 1965, NASA-TN-2870. Effect of high-velocity fluid flow on the bending vibrations and static divergence of a simply supported pipe.

4. S. Naguleswaran, and C. J. H. Williams, 1968, Journal of Mechanical Engineering Science, 10, 228-238. Lateral vibration of a pipe conveying a fluid.

5. M. J. Pettigrew and D. J. Gorman, International Symposium on Vibration Problems in Industry, 1973, Keswick, England. Experimental studies on flow induced vibration to support steam generator design.

6. L. I. Mirowitz, et al., 1962, Aerospace Industries Association of America Report ARTC-32. Panel flutter survey and design criteria.

7. M. P. Paidoussis and J. P. Denise, 1971, Journal of Sound and Vibration, 16, 459-461. Flutter of cylindrical shells conveying fluid.

8. D. S. Weaver, 1972, Journal of Sound and Vibration, 22, 247-248. Letters to the editor on the flutter of thin cylindrical shells conveying fluid.

9. G. W. Housner, 1952, Journal of Applied Mechanics, 19, 205-208. Bending vibration of a pipeline containing flowing fluid.

10. M. P. Paidoussis and J. P. Denise, 1972, Journal of Sound and Vibration, 20, No. 1, 9-26. Flutter of a thin cylindrical shell conveying fluid.

11. D. S. Weaver and T. E. Unny, 1973, Journal of Applied Mechanics, 40, No. 1, 48-52. On the dynamic stability of fluid conveying pipes.

12. R. H. Long Jr, 1955, Journal of Applied Mechanics, 22, 65-68. Experimental and theoretical study of transverse vibration of a tube containing flowing fluid.

13. T. B. Benjamin, 1961, Proceedings of the Royal Society of London, 261, 457-499. Dynamics of a system of articulated pipes conveying fluid, part I and part II.

14. R. W. Gregory and M. P. Paidoussis, 1966, Proceedings of the Royal Society of London, 293, Series A, 512-542. Unstable oscillation of tubular cantilevers conveying fluid, part I-Theory, part II-Experiment.

15. Shoei-Sheng Chen, Vibration Conference and the International Design Automation Conference, 1971, Toronto, Canada, Flow-induced instability of an elastic tube.

16. J. Kempner, 1955, Journal of Applied Mechanics, 22, No. 1, Trans. ASME, 77, 117-118. Remarks on Donnell's Equations.

17. D. S. Weaver and T. E. Unny, 1970, Journal of Applied Mechanics, 37, No. 3, 823-827. The hydroelastic stability of a flat plate.

18. W. Hahn, The Theory and Application of Liapunov's Direct Method, Prentice-Hall, N.J., 1963.

19. N. J. Hoff, 1955, Journal of Applied Mechanics, 22, No. 3, Trans. ASME, 77, 329-334. The accuracy of Donnell's equation.

20. D. S. Weaver, 1969, Ph.D Thesis, University of Toronto. The hydroelastic stability of a flat plate.

21. G. Herrmann and R. W. Bungay, 1964, Journal of Applied Mechanics, 31, 435-440. On the stability of elastic systems subjected to nonconservative forces.

22. J. Dugundji, E. H. Dowell and B. Perkin, 1963, American Institute of Aeronautics and Astronautics Journal, 1, 1146-1154. Subsonic flutter of panels on continuous elastic foundations.

23. K. Forsberg, 1964, AIAA, vol. 2, No. 12, 2150-2157. Influence of boundary conditions on the modal characteristics of thin cylindrical shells.

24. S. E. Widnall and E. H. Dowell, 1967, Journal of Sound and Vibration 6, No. 1, 71-85. Aerodynamic Forces on an oscillating cylindrical duct with an internal flow.

25. M. Holt and S. L. Strack, 1961, Journal of the Aerospace Sciences, 28, 197-208. Supersonic panel flutter of a cylindrical shell of finite length.

26. E. H. Dowell and S. E. Widnall, 1966, AIAA Journal 4, No. 4, 607-610. Generalized aerodynamic forces on an oscillating cylindrical shell: Subsonic and supersonic flow.

27. R. L. Bisplinghoff, H. Ashley and R. L. Halfman, Aeroelasticity, Addison-Wesley Publishing Company, Inc., 1957.

28. T. Karman and M. A. Biot, Mathematical Methods in Engineering, McGraw-Hill Book Company, Inc., 1940.

29. Horst Leipholz, 1970, Stability Theory, New York, Academic Press.

30. H. Kraus, 1967, Thin Elastic Shells, New York, Wiley and Sons.

31. G. Birkhoff, 1960, Hydrodynamics, 2nd Edition, Princeton, New Jersey, Princeton University Press.

32. A. M. Whitman, 1972, Journal of Applied Mechanics, 39, No. 4., 1047-1049. Aspect ratio effects on added-mass of a slender pulsating cylinder.

33. C. M. Blow, 1971, Rubber Technology and Manufacture: Butterworths, London.

APPENDIX I

NOMENCLATURE

c = complex frequency = ω/ω_o

C_p = generalized coordinate

D = flexural stiffness $\frac{Eh^3}{12(1-\nu^2)}$

E = modulus of elasticity

F_{ipq} = $i = 1,2$ improper integrals

h = thickness of shell

H = thickness ratio = h/R

i = $\sqrt{-1}$

I = moment of inertia of thin cylinder $= \pi R^3 h$

$I_n(kr)$ = modified Bessel function of first kind

k^2 = separation constant

ℓ = length of shell

m = mass of fluid per unit length of shell $= \alpha \pi R^2 \rho_o$

n = circumferential mode number

p = axial mode number

p_d = dynamic pressure

R = radius of shell

t = dimensionless integration constant or time

U = flow velocity

V = dimensionless flow velocity

$$= U\sqrt{\frac{12(1-\nu^2)}{\pi^2 E}}$$

w = radial deflection of shell

β = mass ratio = $\frac{\rho_o}{\rho_m}$

δ_{pq} = Kronecker delta

ν = Poisson's data

λ = length of ratio = $\ell/\pi R$

ρ_m = density of shell material

ρ_o = density of fluid

ϕ = perturbation velocity potential

ω = frequency

ω_o = reference frequency = $\frac{\pi^2}{\ell^2}\left(\frac{D}{\rho_m h}\right)^{1/2}$

∇^4 = $\left(\frac{\partial^2}{\partial x^2} + \frac{1}{R^2}\frac{\partial^2}{\partial \theta^2}\right)^2$

∇^{-4} = inverse of ∇^4, $\nabla^4\nabla^{-4} = 1$

APPENDIX II

TABLE OF INTEGRAL F_{1pq} AND F_{2pq} VALUES

F_{111}

n =	1	2	3	4	5	6
λ = 1	.00076191	.00050707	.00038594	.00031213	.00026187	.00022532
2	.00053080	.00031807	.00022750	.00017670	.00014419	.00012164
3	.00040642	.00022939	.00015943	.00012189	.00009852	.00008261
4	.00032753	.00017830	.00012210	.00009267	.00007459	.00006239
5	.00027321	.00014536	.00009872	.00007463	.00005995	.00005078
7	.00020386	.00010516	.00007120	.00005363	.00004300	.00003588
10	.00014665	.00007478	.00005011	.00003767	.00003017	.00002515
15	.00009936	.00005014	.00003350	.00002516	.00002013	.00001678
20	.00007497	.00003768	.00002515	.00001888	.00001511	.00001259
30	.00005020	.00002516	.00001678	.00001259	.00001007	.00000840
45	.00003353	.00001679	.00001119	.00000840	.00000672	.00000560

P_{211}

n = 0	1	2	3	4	5	6
λ = 1	.00468158	.00406339	.00355363	.00313428	.00278758	.00250110
2	.00438225	.00325311	.00255440	.00208559	.00175340	.00150778
3	.00392052	.00260238	.00192372	.00151558	.00124585	.00105549
4	.00346256	.00213103	.00152255	.00117829	.00095858	.00080684
5	.00305982	.00178905	.00125258	.00095986	.00077661	.00065147
7	.00243580	.00134030	.00091869	.00069718	.00056111	.00046924
10	.00183020	.00096510	.00065285	.00049258	.00039527	.00032983
15	.00127460	.000653921	.00043888	.00032992	.00026430	.00022042
20	.00097199	.00049332	.00033000	.00024789	.00019846	.00016546
30	.00065610	.00033014	.00022047	.00016547	.00013242	.00011038
45	.00043989	.00022052	.00014712	.00011038	.00008832	.00007360

$F_{112} = F_{121}$

λ = 1	n = 1	2	3	4	5	6
1	.00016315	.00010265	.00007511	.00005899	.00004835	.00004090
2	.00010671	.00005973	.00004111	.00003119	.00002507	.00002094
3	.00007797	.00004127	.00002784	.00002093	.00001676	.00001399
4	.00006074	.00003128	.00002094	.00001572	.00001258	.00001049
5	.00004944	.00002512	.00001677	.00001258	.00001006	.00000839
7	.00003577	.00001796	.00001198	.00000896	.00000719	.00000599
10	.00002515	.00001258	.00000839	.00000629	.00000503	.000004199
15	.00001677	.00000839	.00000559	.00000419	.00000335	.000002799
20	.00001258	.00000629	.00000419	.00000314	.00000252	.00000210
30	.00000836	.00000419	.00000279	.00000210	.00000168	.00000140
45	.00000559	.00000279	.00000186	.00000140	.00000111	.00000093

F_{122}

n =	1	2	3	4	5	6
λ = 1	.00004171	.00002708	.00002052	.00001670	.00001407	.00001231
2	.00002819	.00001702	.00001247	.00000992	.00000826	.00000708
3	.00002151	.00001260	.00000907	.00000711	.00000584	.00000496
4	.00001753	.00001007	.00000714	.00000553	.00000451	.00000380
5	.00001488	.00000839	.00000588	.00000452	.00000366	.00000308
7	.00001488	.000006284	.00000433	.00000329	.00000265	.00000222
10	.00000857	.000004544	.00000309	.00000233	.00000187	.00000156
15	.000005989	.000003091	.00000208	.00000157	.00000125	.00000105
20	.00000458	.000002337	.00000157	.00000118	.000000943	.000000786
30	.000003105	.000001567	.00000105	.000000786	.000000629	.000000524
45	.00000209	.000001047	.000000699	.000000524	.00000040	.00000035